THESIS FOR THE DEGREE OF LICENTIATE OF ENGINEERING

Towards Practical Implementation of Phase-Sensitive Amplifier Based Transmission Systems

Samuel L. I. Olsson

Photonics Laboratory
Department of Microtechnology and Nanoscience - MC2
CHALMERS UNIVERSITY OF TECHNOLOGY
Göteborg, Sweden, 2013

Towards Practical Implementation of Phase-Sensitive Amplifier Based Transmission Systems

Samuel L. I. Olsson

Göteborg, August 2013

Chalmers University of Technology
Department of Microtechnology and Nanoscience - MC2
Photonics Laboratory
SE-412 96 Göteborg, Sweden
Phone: +46 (0) 31 772 1000

ISSN 1652-0769
Technical Report MC2 - 260

Printed by Bibliotekets reproservice, Chalmers University of Technology
Göteborg, Sweden, August, 2013

Towards Practical Implementation of Phase-Sensitive Amplifier Based Transmission Systems

Samuel L. I. Olsson

Photonics Laboratory
Department of Microtechnology and Nanoscience - MC2
Chalmers University of Technology, SE-412 96 Göteborg, Sweden

Abstract

All commercially available optical amplifiers are so-called phase-insensitive amplifiers (PIAs) which degrade the signal-to-noise ratio (SNR) through the amplification process. This kind of amplifier has a quantum limited noise figure (NF) of 3 dB. Another category of amplifiers are phase-sensitive amplifiers (PSAs) which in theory are capable of noiseless amplification, i.e. amplification with a 0 dB NF. Successful implementation of PSAs in transmission systems would lead to significant performance improvements compared to using conventional PIAs. However, the implementation is challenging and no system with wavelength division multiplexing (WDM) compatibility has previously been demonstrated over a significant transmission distance.

This thesis is dedicated to realizing and investigating the properties of PSA-amplified transmission links utilizing fiber optical parametric amplifiers (FOPA) and the so-called copier-PSA scheme. One of the main challenges on the way towards realization is to recover and amplify a weak phase-modulated wave with high fidelity. To handle this, a hybrid injection locking (IL)/Erbium-doped fiber amplifier (EDFA)-based pump recovery system was designed and thoroughly investigated experimentally. Other challenges include continuous phase-locking of several waves and high-precision wave tuning.

A single-span PSA-amplified transmission link with WDM compatibility was demonstrated over 80 km of fiber. The link performance was compared against a conventional EDFA-based link for operation both in the linear and nonlinear transmission regime. The PSA-amplified system is shown to have capability to mitigate nonlinear distortions due to the Kerr effect and outperform the EDFA-amplified link in both regimes.

Keywords: fiber nonlinearities, fiber optic parametric amplification, four-wave mixing, nonlinear optical signal processing, optical injection locking, phase-sensitive amplification

List of papers

Appended publications

This thesis is based on work contained in the following papers:

[A] **S. L. I. Olsson**, B. Corcoran, C. Lundström, E. Tipsuwannakul, S. Sygletos, A. D. Ellis, Z. Tong, M. Karlsson, and P. A. Andrekson "Injection locking-based pump recovery for phase-sensitive amplified links," Optics Express **21**, 14512–14529 (2013).

[B] B. Corcoran, **S. L. I. Olsson**, C. Lundström, M. Karlsson, and P. Andrekson, "Phase-sensitive Optical Pre-Amplifier Implemented in an 80km DQPSK Link," in Optical Fiber Communication Conference and Exposition (OFC) and National Fiber Optic Engineers Conference (NFOEC), Technical Digest (CD) (Optical Society of America, 2012), Post-deadline paper PDP5A.4.

[C] **S. L. I. Olsson**, B. Corcoran, C. Lundström, M. Sjödin, M. Karlsson, and P. A. Andrekson, "Phase-Sensitive Amplified Optical Link Operating in the Nonlinear Transmission Regime," in European Conference and Exhibition on Optical Communication (ECOC), Technical Digest (CD) (Optical Society of America, 2012), paper Th.2.F.1.

Other publications

The following papers has been published or been accepted for publication but are not included in the thesis. The content partially overlap with the appended papers or is out of the scope of this thesis.

[D] **S. L. I. Olsson**, B. Corcoran, C. Lundström, E. Tipsuwannakul, S. Sygletos, A. D. Ellis, Z. Tong, M. Karlsson, and P. A. Andrekson "Optical Injection-Locking-Based Pump Recovery for Phase-Sensitively Amplified Links," in Optical Fiber Communication Conference and Exposition (OFC) and National Fiber Optic Engineers Conference (NFOEC), Technical Digest (CD) (Optical Society of America, 2012), paper OW3C.3.

[E] C. Lundström, B. Corcoran, **S. L. I. Olsson**, Z. Tong, M. Karlsson, and P. A. Andrekson, "Short-Pulse Amplification in a Phase-Sensitive Amplifier," in Optical Fiber Communication Conference and Exposition (OFC) and National Fiber Optic Engineers Conference (NFOEC), Technical Digest (CD) (Optical Society of America, 2012), paper OTh1C.1.

[F] T. Richter, B. Corcoran, **S. L. I. Olsson**, C. Lundström, M. Karlsson, C. Schubert, and P. A. Andrekson, "Experimental Characterization of a Phase-Sensitive Four-Mode Fiber-Optic Parametric Amplifier," in European Conference and Exhibition on Optical Communication (ECOC), Technical Digest (CD) (Optical Society of America, 2012), paper Th.1.F.1.

[G] L. Grüner-Nielsen, D. Jakobsen, S. Herstrøm, B. Pálsdóttir, S. Dasgupta, D. Richardson, C. Lundström, **S. L. I. Olsson**, and P. A. Andrekson, "Brillouin Suppressed Highly Nonlinear Fibers," in European Conference and Exhibition on Optical Communication (ECOC), Technical Digest (CD) (Optical Society of America, 2012), paper We.1.F.1.

[H] C. Lundström, R. Malik, L. Grüner-Nielsen, B. Corcoran, **S. L. I. Olsson**, M. Karlsson, and P. A. Andrekson, "Fiber Optic Parametric Amplifier With 10-dB Net Gain Without Pump Dithering," IEEE Photonics Technology Letters **25**, 234-237 (2013).

[I] C. Lundström, **S. L. I. Olsson**, B. Corcoran, M. Karlsson, and P. A. Andrekson, "Phase-Sensitive Amplifiers for Optical Links," in Optical Fiber Communication Conference and Exposition (OFC) and National Fiber Optic Engineers Conference (NFOEC), Technical Digest (CD) (Optical Society of America, 2013), paper OW3C.5.

[J] B. Corcoran, **S. L. I. Olsson**, C. Lundström, M. Karlsson, and P. A. Andrekson, "Mitigation of Nonlinear Impairments on QPSK Data in Phase-Sensitive Amplified Links," Accepted to European Conference and Exhibition on Optical Communication (ECOC), Technical Digest (CD) (Optical Society of America, 2013)

[K] C. Lundström, R. Malik, A. L. Riesgo, B. Corcoran, **S. L. I. Olsson**, M. Karlsson, and P. A. Andrekson, "Fiber-optic Parametric Amplifiers Without Pump Dithering," Accepted to 3rd Workshop on Specialty Optical Fiber and Their Applications, 2013

Acknowledgement

First and foremost I would like to thank my supervisors Peter Andrekson and Magnus Karlsson for accepting me as a PhD student, their guidance and support, and for being good role models. Bill Corcoran deserves special thanks for good collaboration and his contributions to the publications in this thesis. It has been a pleasure working with such a skilled, efficient, and enthusiastic person. I will always remember our intense work together in the lab before the deadlines.

Carl Lundström also deserves special thanks for helping to solve many of the everyday issues, sharing his expertise and knowledge, and for his contributions to the papers. I am very grateful to Tong Zhi for always taking time to answer my questions and for being a good source of inspiration through the impressive work he carried out while he was working at the photonics laboratory.

Ekawit Tipsuwannakul and Pontus Johannisson should be thanked for sharing their expertise and always being willing to help. Martin Wahlsten deserves thanks for giving me a good introduction when I just started my PhD studies, coming to the laboratory without any prior knowledge of fiber optics.

I would like to express my gratitude to Andrew Ellis for letting me spend time at Tyndall National Institute in Cork, Ireland and Stylianos Sygletos for teaching me about phase-locked loops and injection locking during the visit. When working long hours it is important to fit in some breaks. The number one break activity has been to play ping pong and I want to thank, especially Martin Sjödin, but also Tobias Eriksson and Yuxin Song for many great ping pong games.

I would also like to thank the whole photonics laboratory and visiting researches that have been in the group for creating a nice working environment.

Last but not least, I would like to thank my family and friends.

Samuel L. I. Olsson

Göteborg
August 2013

This work was financially supported by the European Commission STREP Project PHASORS (FP7-ICT-2007-2 22457), the European Research Council Advanced Grant PSOPA (291618), the Knut and Alice Wallenberg Foundation, and also by the Swedish Research Council (VR).

List of Acronyms

16QAM 16-ary quadrature amplitude modulation 7, 45

AOM acousto-optic modulator 34
AQN amplified quantum noise 25
ASE amplified spontaneous emission 8, 10, 25, 32, 43

BER bit error ratio 47

CD chromatic dispersion 5
CW continuous wave 20, 31, 32

DFA doped fiber amplifier 7, 8
DFB distributed feedback 42
DQPSK differential quadrature phase-shift keying 37, 47
DSP digital signal processing 38

EDFA erbium-doped fiber amplifier 1, 3–5, 7–10, 20, 21, 31, 32, 37, 38, 45, 47, 48

FEC forward error correction 2
FOPA fiber optical parametric amplifier 3, 4, 7, 19–21, 23, 24, 27, 31, 38
FWM four-wave mixing 3, 19–25, 31, 32

HDTV high-definition television 2
HNLF highly nonlinear fiber 31, 32

ICT information and communication technology 1, 2
IL injection locking 41, 42, 47

ML master laser 42, 43

NF noise figure 3, 5, 8–10, 12–17, 19, 21, 28, 30, 31, 35–37, 47

OIL optical injection locking 4, 38, 41–43

OOK on-off keying 7
OPC optical phase conjugation 38
OSNR optical signal-to-noise ratio 6

PC polarization controller 32
PI phase-insensitive 3, 15–17, 19, 20, 24, 28, 29, 33–36
PI-FOPA phase-insensitive fiber optical parametric amplifier 21, 32
PIA phase-insensitive amplifier 3, 5–8, 14–16, 28, 30, 33, 35–37
PLL phase-locked loop 39
PM-QPSK polarization-multiplexed quadrature phase-shift keying 7
PMD polarization-mode dispersion 5
PS phase-sensitive 3, 16, 17, 19, 20, 24, 28–30, 33–36
PS-FOPA phase-sensitive fiber optical parametric amplifier 3, 4, 19, 21
PSA phase-sensitive amplifier 3–5, 7, 15–17, 28, 30, 33–39, 41, 45, 47, 48

RF radio frequency 12, 47
RIN relative intensity noise 42

SBS stimulated Brillouin scattering 31, 32, 45
SHG second harmonic generation 20
SL slave laser 42, 43
SNR signal-to-noise ratio 2, 3, 5, 12, 13, 30, 37, 48
SOA semiconductor optical amplifier 7, 9, 10
SOP state of polarization 39, 42
SPM self-phase modulation 6, 22, 23, 38
SRS stimulated Raman scattering 10, 31
SSMF standard single mode fiber 9, 22, 31

VOA variable optical attenuator 43

WDM wavelength division multiplexing 2, 4, 6–10, 32–35, 37, 39, 45

XPM cross-phase modulation 6, 22, 23, 38

ZDW zero-dispersion wavelength 20, 31

Contents

Chapter 1
Introduction

From the beginning of mankind inventions and technical advances have driven our development and formed the world we live in. Today's society is to a large extent shaped by the information and communication technology (ICT) that emerged in the 1990's. The ICT has had a profound impact on everyday life, for instance through enabling services that make information more accessible and providing new means for communication and media consumption. The ICT has also contributed to large scale trends such as globalization by making distance less of a boundary. Based on the global interest in ICT related services it is most likely that what we have seen so far is only the beginning of the ICT era.

The key enabling technology for the ICT was the long-haul fiber optical communication system, making it possible to transmit information at high speed over intercontinental distances. The long-haul fiber optical communication system was in turn realized based on a number of inventions and technical advances of the last century. The most important components were the laser [1], the low-loss optical fiber [2], and the erbium-doped fiber amplifier (EDFA) [3]. If the ICT can continue to develop, depends to a large extent on today's innovations and technical advances.

The main topic of this thesis concern a novel optical amplification system that can potentially improve the performance of long-haul fiber optical communication systems and through this lead to continued development in the area of ICT.

Chapter outline

In section 1.1 we place this work in a context and give a motivation to why the work is of interest to the general community. In section 1.2 the motivation for each appended paper is described in detail. Finally, in section 1.3 we outline the structure and content of the thesis.

1.1 Background

The development of services in the area of ICT goes hand in hand with an increased demand for capacity in the fiber optical communication systems. Particularly capacity intensive services are those in the field of home entertainment, where rapid advancements in display technology and technical solutions for distribution over internet push the demand. New standards, where current examples are ultra high-definition television (HDTV), with up to sixteen times the pixel count of standard HDTV, and 3D television, will increase the demand for capacity. Another field is business and productivity related services where e.g. cloud computing, cloud storage, and virtual meetings will contribute to an increased demand. Additionally, the number of people and devices connected to internet is expected to grow which will also add to the demand.

The current state-of-the-art long-haul fiber optical transmission systems are the result of four decades of development and technological advances. One of the first commercial systems, deployed in 1977, operated at 45 Mb/s over a distance of 2.6 km [4]. This should be compared to current state-of-the-art field experiments were data is transmitted at 40.5 Tb/s over 1 822 km [5]. This capacity increase of almost six orders of magnitude and considerable reach extension has been accomplished by implementing techniques such as wavelength division multiplexing (WDM), i.e. simultaneously transmitting information at several wavelengths, forward error correction (FEC), and advanced modulation formats [6]. Although the technology has progressed the basic building blocks of a long-haul fiber optical transmission system are still the same.

A long-haul fiber optical communication system consists of a transmitter, optical fiber spans, and a receiver. The function of the transmitter is to generate an optical signal encoded with the data that should be transmitted. The optical fiber guide the light between the origin and the destination. Despite the extremely low attenuation that can be achieved in optical fibers, with the current record being 0.149 dB/km [7], periodic amplification is needed to compensate for the attenuation. The receiver finally detect the transmitted signal and recover the data.

The capacity (bit/s) of a communication system can be defined as the product of the spectral efficiency (bit/s/Hz), a measure of how efficient the spectrum is used, and the signal bandwidth (Hz). In general terms the capacity can be increased if the signal-to-noise ratio (SNR) at the receiver is increased [8]. Higher SNR at the receiver can e.g. enable usage of modulation formats with higher spectral efficiency.

The SNR at the receiver in a long-haul fiber optical communication system can be increased by boosting the signal power at the output of the transmitter or by reducing the noise added by the optical amplifiers. The latter can be done either by improving the noise performance of the individual amplifies or by reducing the spacing between the amplifiers, thus increasing the total number of amplifiers. Increasing the number of amplifiers is in general not preferred due to higher cost

and focus is instead on improved noise performance.

The noise added to a signal by an optical amplifier is quantified by the amplifier noise figure (NF), defined as the ratio of the input SNR to the output SNR. All commercial optical amplifiers available today are so-called phase-insensitive amplifiers (PIAs), meaning that the gain is independent of the signal phase. This kind of amplifier has a 3 dB quantum-limited NF at high gain [9]. In current long-haul fiber optical communication systems the most commonly used amplifier is the EDFA, a PIA. The lowest NF that has been experimentally demonstrated for an EDFA is 3.1 dB [10].

Another class of amplifiers are phase-sensitive amplifiers (PSAs), for which the gain is dependent on the signal phase. The quantum-limited NF for this kind of amplifier is 0 dB [11], which in practice mean noiseless amplification. Successful implementation of a low NF amplifier in a long-haul fiber optical communication system would have major implications due to the large reduction in SNR degradation through the transmission link. The improvement in SNR could either be used for increasing the capacity or extending the reach.

As mentioned earlier there are several techniques implemented in today's long-haul fiber optical communication systems for increasing capacity. Some of these techniques place requirements on the optical amplifiers in the link. It is, e.g., crucial that the amplifiers are able to amplify several wavelength channels simultaneously over a wide bandwidth and in the range where the optical fiber has low loss, that they are modulation format, symbol rate, and polarization independent, as well as capable of low-noise, high-gain, and flat-gain operation, with high gain efficiency. The EDFA is the amplification technology that best satisfy these requirements and thus has become widely used. However, the EDFA is not the perfect amplification technology. For example, the bandwidth of EDFAs is fairly limited and the SNR will always be degraded by at least 3 dB. The problem with limited bandwidth has to some extent been solved by combining EDFAs with Raman amplifiers in hybrid amplification systems [12, 13].

Fiber optical parametric amplifiers (FOPAs) can be operated in both phase-insensitive (PI)- and phase-sensitive (PS)-mode and has proved to be a promising amplification technology. FOPAs rely on four-wave mixing (FWM) where several waves interact to provide gain through parametric amplification and are most notably capable of high gain, with the current record being 70 dB [14], wide bandwidth [15], and noiseless amplification when operated in PS-mode. In some aspects FOPAs show better performance than EDFAs, although from a practical point of view, also taking cost into consideration, EDFAs are still the most attractive optical amplification technology.

Phase-sensitive fiber optical parametric amplifiers (PS-FOPAs) can be either frequency-degenerate or frequency-nondegenerate depending on how the wavelengths of the interacting waves are chosen. Frequency-nondegenerate PS-FOPAs are capable of simultaneous amplification of many wavelength channels but have historically been difficult to implement due to strict requirements on phase-locking

of the interacting waves. In 2005 the so-called copier-PSA scheme was proposed and provided a satisfactory solution to the problem of phase-locking the waves [16]. This scheme made it possible to design multi-channel, modulation format independent [17], PSA-amplified links.

There have been some studies of PS-FOPA-amplified transmission links but none including both a significant length of transmission fiber and featuring the capability of modulation format independent operation. Thus, up until now there have been no convincing demonstrations of PSA-amplified transmission links.

1.2 Motivation

The motivation behind this thesis work has been to demonstrate a modulation format independent and WDM compatible PSA-amplified transmission link, implemented using a PS-FOPA, over a significant length of fiber and with better performance than a comparable EDFA-amplified transmission link.

In [Paper A] we take the first step towards realizing a PSA-amplified transmission link by demonstrating a hybrid optical injection locking (OIL)/EDFA-based pump recovery system, a necessary part of a long span PSA-amplified link. The system we demonstrate is capable of enabling PSA-amplified links with more than 200 km long spans. The operating limit of the system is thoroughly investigated. In [Paper B] we use the pump recovery system to demonstrate the longest modulation format independent and WDM compatible PSA-amplified transmission link ever reported. We compare the performance to an EDFA-amplified link and show better performance for the PSA-amplified link.

From the perspective of capacity, an interesting limit for all transmission systems is the limit of high signal power launched into the fiber span. In [Paper C] we characterize the previously demonstrated PSA-amplified transmission link in the regime of nonlinear transmission.

1.3 Thesis outline

In chapter 2 we introduce the topic of optical amplification and discuss the noise limits of optical amplifiers. In chapter 3 we describe FOPAs, the amplification technology that this thesis work is based on, in detail. In chapter 4 the implementation of PSAs in transmission links is discussed along with the properties of these links. The scheme for realizing a long span PSA-amplified link rely on OIL. The concept of OIL is briefly introduced in chapter 5. In chapter 6 future topics of research, building upon what is presented in this thesis, are presented. In the final chapter, chapter 7, the appended papers are summarized.

Chapter 2
Amplification and noise limits

The maximum attainable capacity in a communication system is related to the signal SNR before the receiver. In a long-haul fiber optical communication system this is mainly governed by the noise properties of the link amplifiers. The increasing demand for capacity thus makes optical amplifier noise an important topic.

All conventional optical amplifiers, including the very common EDFA, are PIAs with a 3 dB quantum limited NF. PSAs on the other hand have a 0 dB quantum limited NF, which in practice mean noiseless amplification.

Chapter outline

The purpose of this chapter is to give an introduction to optical amplification and to provide an understanding of the different noise properties in PIAs and PSAs. To this end, in section 2.1 we introduce the topic of optical amplification along with the most common amplification techniques. The fundamental limit to the noise added by an amplifier is determined by quantum mechanics. In section 2.2 we discuss the quantum noise limits for PIAs and PSAs. Finally, in section 2.3 we discuss how amplifier noise impacts the performance in multi-span links.

The material presented in this chapter is essential for understanding the motivation behind the work in [Paper B], where the target was to demonstrate a PSA-amplified link that outperform a conventional EDFA-amplified link.

2.1 Optical amplification

2.1.1 Introduction

Propagating a signal through an optical fiber will unavoidably lead to attenuation and distortion of the signal. The distortion can either be due to linear or nonlinear effects occurring in the optical fiber. Linear effects, such as chromatic dispersion (CD) and polarization-mode dispersion (PMD), are independent of the

signal power and are always present. These effects are in general easier to mitigate than nonlinear effects, such as self-phase modulation (SPM) and cross-phase modulation (XPM), which depend on the signal power and manifest at high powers or long transmission distances.

A communication system relies on that the transmitted data can be accurately recovered at the end of the link. In practice this means that the signal cannot be too distorted by linear and nonlinear effects and that the power at the receiver is high enough so that the signal can be received without adding excessive noise. The naive solution to satisfy this power condition would be to increase the power launched into the link. However, this would increase the nonlinear distortions of the signal and is therefore, in most cases, not a viable path. Instead, the optical power has to be managed throughout the link so that the power condition at the receiver is satisfied without reaching too high signal power and then induce nonlinear distortion at any given point in the link.

From the early years of long-haul fiber optical communication systems up until the mid 90's fiber loss was mostly managed by periodically detecting and retransmitting the signal using optoelectronic repeaters. Using repeaters was not a practical solution for loss management in WDM systems since one receiver-transmitter pair is needed for each wavelength channel, resulting in a complex and expensive system. With the introduction of WDM an alternative loss management technique was therefore required and optical amplification, capable of simultaneous amplification of many channels, became the mainstream method.

2.1.2 Amplifier noise

Optical amplification is associated with degradation of the signal quality due to noise added by the amplifier. Without taking the receiver into account the quality of the signal can be quantified by the optical signal-to-noise ratio (OSNR) measure, specifying the ratio between the signal power and the noise power in a given bandwidth. Since both the signal and the noise at the input of an amplifier is amplified the OSNR would not degrade if the amplifier did not add any excess noise. However, in many cases, the amplifier has independent internal noise that is added to the signal, thus leading to degraded OSNR.

In multi-span transmission links, i.e. links with many cascaded amplifiers, the noise added by the amplifiers accumulate throughout the link and successively reduce the OSNR. For a communication system the signal OSNR is strongly related to the attainable capacity [18], with higher OSNR enabling higher capacity. The noise properties of the amplifiers is therefore very important when designing a communication system.

Common for all commercially available optical amplifiers is that they are PIAs, i.e. their gain is independent of the signal phase. Moreover, they are generally operated in a linear regime, i.e. where the output signal is linearly related to the input signal. Working in the linear regime is preferred since working in a nonlinear

regime would induce signal distortions.

The ultimate limit to how much noise is added by an optical amplifier is governed by quantum mechanics. It has been shown that all PIAs operating in the linear regime with a gain $G > 1$ must add noise to the signal since a noise-free amplifier would violate Heisenberg's uncertainty principle [19, 20]. PSAs on the other hand, for which the gain is dependent on the signal phase, can in theory amplify a signal without adding any noise [11]. This property of noiseless amplification make PSAs very interesting for transmission system applications.

2.1.3 System requirements

In today's long-haul fiber optical communication systems WDM is one of the most important techniques for increasing capacity. It is thus essential that the optical amplifiers in the link can provide gain (> 20 dB) over large bandwidths. Furthermore, it is important that the gain is flat over the signal bandwidth since gain differences between the channels would accumulate into large power differences.

Traditionally on-off keying (OOK) has been the most commonly used modulation format in optical communication systems. However, the trend is moving towards using more advanced modulation formats with higher spectral efficiency, such as polarization-multiplexed quadrature phase-shift keying (PM-QPSK) and 16-ary quadrature amplitude modulation (16QAM). This requires the amplifiers to be polarization independent, modulation format independent, and have small signal distortion.

As for all systems energy consumption and cost is important. It is therefore important that the amplifier has a high gain efficiency, i.e. low pump power requirement per dB of gain. Furthermore, to reduce the energy consumption and cost, a primary concern when designing a communication system is to minimize the transmission loss. In a fiber optical communication system the loss originate mainly from attenuation in the optical fiber. The loss is wavelength dependent and the range which has the lowest loss is called the conventional 'C'-band and spans from 1530 to 1570 nm in silica fibers. It is thus important that the amplifier is capable of amplification in the C-band.

Several types of optical amplifiers, capable of amplification in the C-band, are commercially available. The most common types are doped fiber amplifiers (DFAs), with the EDFA [21] being the dominating technology, Raman amplifiers [22], semiconductor optical amplifiers (SOAs) [23], and FOPAs [15]. These amplifiers are based on different gain mechanisms and have different performance and properties.

2.1.4 Amplification techniques

Erbium-doped fiber amplifiers

The EDFA is the dominating technology for loss management in today's long-range fiber optical communication systems. The EDFA was invented in 1986 [3], and quickly became an interesting technology due to its capability to amplify signals in the C-band. After its commercialization in the mid-1990s it rapidly gained its position as the leading loss management technology.

The EDFA, with a bandwidth of about 40 nm (5.3 THz), is mainly used for C-band operation but longer 'L'-band (1570-1610 nm) operation has been demonstrated by increasing the erbium concentration [24], and shorter 'S'-band (1490-1520 nm) operation by using a double-pass configuration [25]. DFAs operating in the S-band (1480-1510 nm) can also be constructed by doping with thulium instead of erbium [26].

All DFAs are optically pumped and amplification is achieved through population inversion, i.e. the majority of the ions are in an excited state, and stimulated emission. Along with the stimulated emission there is also spontaneous emission. The spontaneously emitted photons will be amplified and result in amplified spontaneous emission (ASE). The ASE will then beat with the signal at detection and cause noise, which is the main noise source associated with EDFAs.

The amount of ASE noise generated in an EDFA is affected by the pump wavelength and the pumping scheme. Pumping can be done at 980 and 1480 nm, with 980 nm pumping giving better noise performance. The pumping schemes commonly employed are unidirectional pumping in the forward or backward direction and bidirectional pumping.

Apart from the capability of C-band operation, the EDFA has many other valuable features. The gain mechanism in EDFAs results in a very slow gain response time, on the order of milliseconds. This feature makes of possible to operate EDFAs in gain saturation mode without inducing signal distortion and channel crosstalk in WDM systems, i.e. they can work as linear amplifiers on a bit level even if the gain is saturated on average.

From a long-haul transmission system perspective other important features are polarization insensitivity and high gain, a high gain efficiency, ~ 0.1 mW pump power required per dB of gain [27], and low NF, 3.1 dB at 54 dB gain has been demonstrated [10]. Its compatibility with silica fibers and low insertion loss is also important. All these features have contributed to the popularity of the EDFA.

The gain of EDFAs is not dependent on the phase of the signal and EDFAs are therefore PIAs and have a 3 dB quantum limited NF. The actual NF is strongly dependent on the population inversion, with the lowest NF attainable at the highest population inversion. In the high gain limit the NF of an EDFA is given by $\mathrm{NF} = 2n_{\mathrm{sp}}$ where n_{sp} is the spontaneous emission factor which is always greater than or equal to unity [9, p. 100]. For complete medium inversion the spontaneous emission factor equals unity and the NF take the value of 2 (3 dB). In practice the

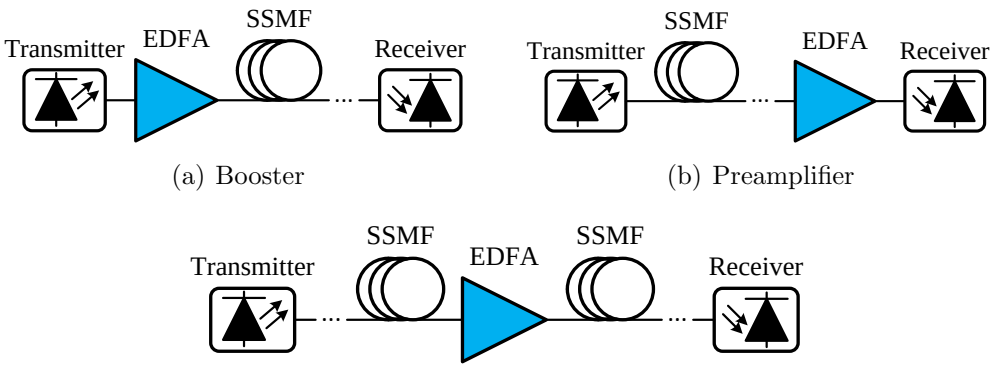

(a) Booster

(b) Preamplifier

(c) In-line amplifier

Figure 2.1: Illustration of possible EDFA implementations. SSMF: standard single mode fiber.

NF exceeds 3 dB and can be as large as 6-8 dB in commercial amplifiers due to other noise sources.

EDFAs, and amplifiers in general, have a few different common usages in fiber optical communication systems. The first usage is as a power booster placed after the optical transmitter to increase the signal level before transmission. Another usage is as a preamplifier placed before the optical receiver where the function is to improve the receiver sensitivity. The last common usage is as in-line amplifier in a long-haul transmission system. The in-line amplifier is used to compensate the loss from the passive fiber sections. The three different usages are illustrated in figure 2.1.

Semiconductor optical amplifiers

SOAs were developed during the 1980s and can provide gain through stimulated emission in an electrically pumped semiconductor. The main advantages of SOAs are modulation format independence, WDM compatibility, low power consumption and compactness. By varying the design SOAs can be made to operate in a range from 0.85 to 1.60 μm with gain bandwidths in the order of 50 nm.

Unfortunately there are several issues with SOAs that make them problematic for use in long-haul transmission systems. A major problem is nonlinearities and crosstalk that distort the signal, especially in WDM systems, which is partly due to picosecond gain response time [28].

Other concerns are coupling losses both into and out of the device due to difference in refractive index and waveguide shape compared to the silica optical fiber. The input coupling loss result in relatively high NFs and the output loss reduce the achievable gain. SOAs with a 7.2 dB NF at 29 dB gain has been demonstrated [29]. Polarization dependent operation is also an issue for SOAs.

Although the SOAs has difficulty to compete with other amplification technologies for applications in long-haul fiber optical communication systems they are still interesting for signal processing applications such as wavelength converters and all-optical regeneration [23].

Raman amplifiers

Raman amplifiers utilize the phenomenon of stimulated Raman scattering (SRS), first discovered in 1962 [30, 31], for signal amplification [22, 27, 32]. Raman scattering [33] is the process when a photon is absorbed by a molecule which then emit a photon of lower frequency than the one absorbed. The energy difference between the absorbed and emitted photon is balanced by a phonon, a vibrational mode of the molecule. The molecule can also emit a photon of higher frequency than the one absorbed but that process is much more uncommon since it requires the presence of a phonon with the correct energy. Raman scattering is a very fast process and takes place on a sub-picosecond timescale.

In a Raman amplifier, which are optical fiber based, two waves are present in the fiber, a strong pump wave that will excite the molecules and a signal wave, at lower frequency, that will be amplified. The gain, originating from SRS, depend on the frequency separation between the pump and the signal, the medium, and the signal and pump polarization, with co-polarized waves providing highest gain. In silica-based fibers the gain bandwidth is about 40 THz and the peak gain occur at about 13 THz. Due to the large bandwidth, Raman amplifiers are attractive for WDM systems that extend outside the C-band.

Raman amplifiers have a fairly low gain efficiency with ~ 10 mW pump power per dB gain. However, high gain can be achieved with up to 45 dB demonstrated [34], and for pump powers above a certain threshold value the signal power builds up almost exponentially. Raman amplifiers are modulation format independent and can be implemented in polarization independent configurations.

They can be implemented both as lumped and distributed amplifiers, i.e. the gain is distributed along the transmission fiber. In general it is attractive to use distributed amplification due to improved noise performance and reduced nonlinear distortion. Combining distributed Raman amplification with EDFAs has also been demonstrated with promising results [12, 13].

Since the amplification is taking place in the transmission fiber itself there are no insertion losses associated with the technique and low NF can be achieved. The dominant noise source for Raman amplifiers is ASE noise from spontaneous Raman scattering.

2.2 Quantum noise limits

2.2.1 Fundamental concepts

Quantum and thermal noise

In contrast to the classical description of electromagnetic fields, quantum mechanics predict that the vacuum state, i.e. the state with no photons, has a non-zero ground-state energy. This energy is called zero-point energy or vacuum energy and has no analogue in the classical theory. The value of the zero-point energy for a single mode with frequency ω_i is $\hbar\omega_i/2$, which follows from a description of the quantized electromagnetic field as composed of infinitely many uncoupled harmonic oscillators [35, p. 139–144].

A more intuitive explanation of the zero-point energy can be obtained by considering the uncertainty principle which state that there is a fundamental limit to the accuracy of a simultaneous measurement of a particles position q and momentum p. The principle is formulated as [36, p. 43]

$$\Delta p \Delta q \geq \frac{\hbar}{2} \tag{2.1}$$

where Δp and Δq are the uncertainties associated with the position and momentum, respectively. Taking the starting point in (2.1) it can be shown that the zero-point energy is the result of zero-point fluctuations in the position q and momentum p of a harmonic oscillator [36, p. 81–82]. With this interpretation of the zero-point energy it is close to define a minimum detectable noise power P_{QN} as

$$P_{\mathrm{QN}} = \frac{\hbar\omega B_0}{2} \tag{2.2}$$

where B_0 is the bandwidth of the detector used to measure the noise. This noise power is often referred to as quantum noise [9, p. 71].

Thermal noise, another fundamental noise source, has the corresponding power [9, p. 71]

$$P_{\mathrm{TN}} = \frac{\hbar\omega B_0}{\exp\left[\dfrac{\hbar\omega}{k_{\mathrm{B}}T}\right] - 1} \tag{2.3}$$

where k_{B} is the Boltzmann constant and T is the temperature in Kelvin. For a system operating at a temperature > 0 K both quantum noise and thermal noise will be present and it is interesting to compare the relative contribution from these two noise sources at various frequencies. In Fig. 2.2 we have plotted the quantum noise and the thermal noise versus frequency at a temperature $T = 290$ K. We clearly see the existence of two regimes. At low frequencies thermal noise is dominating while at high frequencies quantum noise is dominating. The intersection, where thermal noise and quantum noise is equal, depends on the temperature but at $T = 290$

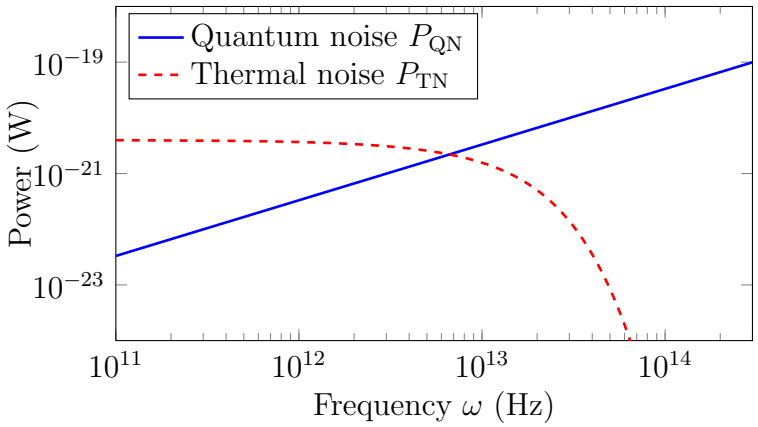

Figure 2.2: Theoretical comparison of quantum noise P_{QN} and thermal noise P_{TN} versus frequency ω at $T = 290$ K.

K (room temperature) is occurs at a frequency of 6.6 THz, corresponding to a wavelength of 45 μm. Reducing the operating temperature will move the crossing to lower frequencies, i.e. extend the region where quantum noise dominate.

The input noise for an electronic amplifier operating at radio frequency (RF) and room temperature will thus be dominated by thermal noise rather than quantum noise. In this case the input signal has large excess noise beyond the quantum limit. This will lead to a negligible SNR degradation through the amplifier, considering only the addition of quantum noise in the amplifier. Amplifiers operating at RF can thus realize NFs arbitrarily close to 1 (0 dB) [37]. A similar situation occurs in multi-span links where the signal carries large excess noise due to previous amplification stages. At frequencies typically used in fiber optical communication systems, i.e. around 1.55 μm (193 THz), it is clear that, in the absence of other external noise sources, quantum noise dominate.

Phasor representation of quantum states

For a qualitative understanding of the quantum noise associated with a signal, it is illustrative to use phasor representation and phasor plots. In the classical description a signal $S = A\sin(\omega t + \phi)$ can be expressed as

$$S = \mathrm{Re}\big[(X_1 + iX_2)\exp(-i\omega t)\big] = X_1\cos(\omega t) + X_2\sin(\omega t) \tag{2.4}$$

where

$$X_1 = A\sin(\phi) \quad \text{and} \quad X_2 = A\cos(\phi) \tag{2.5}$$

are the in-phase and quadrature component of S, respectively. Represented in this form the information is carried by slow variations in X_1 and X_2. Due to the absence of quantum noise in the classical description this signal is represented by an infinitesimal point at (X_1, X_2) in a phasor plot.

In a quantum mechanical description the information of a single mode signal can in an analogous way be related to two operators $\hat{X}_1$ and $\hat{X}_2$ which give the amplitude of the in-phase and quadrature component, respectively. These two operators satisfy the commutation relation [11]

$$\left[\hat{X}_1, \hat{X}_2\right] = \frac{i}{2} \tag{2.6}$$

which in turn implies [38, p. 35] the uncertainty relation

$$\left\langle (\Delta\hat{X}_1)^2 \right\rangle \left\langle (\Delta\hat{X}_2)^2 \right\rangle \geq \frac{1}{16}, \tag{2.7}$$

where $\left\langle (\Delta\hat{X}_i)^2 \right\rangle$ represent the variance of $\hat{X}_i$.

In the classical picture the signal power P is related to the complex amplitude $X_1 + iX_2$ by $P = |X_1 + iX_2|^2 = X_1^2 + X_2^2$. In the same manner we can express the noise power in the quantum mechanical description as $\left\langle (\Delta\hat{X}_1)^2 \right\rangle + \left\langle (\Delta\hat{X}_2)^2 \right\rangle$ and using (2.7) we get the inequality

$$\left\langle (\Delta\hat{X}_1)^2 \right\rangle + \left\langle (\Delta\hat{X}_2)^2 \right\rangle \geq \frac{1}{2}. \tag{2.8}$$

The noise power in (2.8) is expressed in units of number of quanta, i.e. in energy units of $\hbar\omega$, and we note that the minimum value is exactly the zero-point energy $\hbar\omega/2$.

A signal, called a state in the quantum mechanical description, with the uncertainty given by (2.8) can be illustrated in a phasor plot. The quantum state that is most similar to a classical state is the coherent state. This state has the minimum amount of noise allowed by (2.8) and the noise is distributed equally between the in-phase and quadrature component, i.e. $\left\langle (\Delta\hat{X}_1)^2 \right\rangle = \left\langle (\Delta\hat{X}_2)^2 \right\rangle$. A coherent state is shown in figure 2.3(a). The vacuum state, with only the zero-point fluctuations is illustrated in figure 2.3(b) and a so-called squeezed state is illustrated in figure 2.3(c). In the squeezed state the noise is not evenly distributed between the in-phase and quadrature component, i.e. $\left\langle (\Delta\hat{X}_1)^2 \right\rangle \neq \left\langle (\Delta\hat{X}_2)^2 \right\rangle$.

Noise figure

When discussing noise in optical amplifiers we are in general interested in how much noise is added to the signal by the amplifier. To quantify this noise it is convenient to use the NF measure [39]. For amplifiers operating in the linear regime the NF is defined as

$$\mathrm{NF} = \frac{\mathrm{SNR}_{\mathrm{in}}}{\mathrm{SNR}_{\mathrm{out}}} \tag{2.9}$$

where $\mathrm{SNR}_{\mathrm{in}}$ is the SNR at the amplifier input port and $\mathrm{SNR}_{\mathrm{out}}$ is the SNR at the amplifier output port. The SNR is defined as the ratio of the signal power to the noise power, measured using an ideal photodetector with perfect quantum

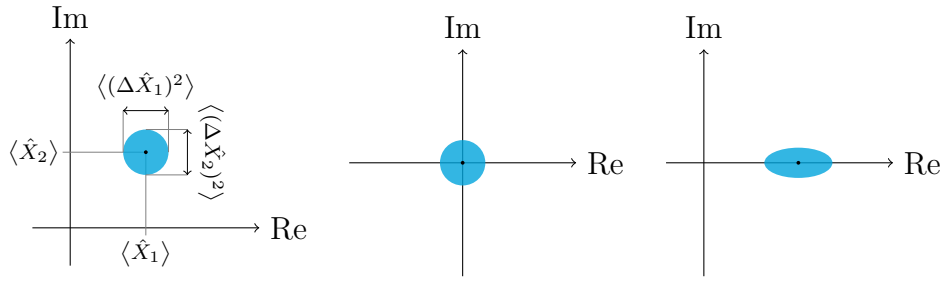

(a) Coherent state (b) Vacuum state (c) Squeezed state

Figure 2.3: Phasor plots of various quantum mechanical states.

efficiency of unity. To ensure that the NF measure has the maximum sensitivity to noise added by the amplifier it is assumed that the input signal is only degraded by shot noise, resulting from the particle nature of light.

2.2.2 Phase-insensitive amplifiers

It was proved already in 1962 by Heffner [19] that a PIA must add noise to the signal. His argument is outlined below. The uncertainty principle (2.1) can be written as a number-phase uncertainty relation [36, p. 77]

$$\Delta n \Delta\phi \geq \frac{1}{2} \tag{2.10}$$

where n denote the average number of photons, related to the amplitude, and ϕ denote the phase. The variables Δn and $\Delta\phi$ represent the uncertainties in n and ϕ, respectively, that are associated with a measurement. The crucial point in Heffner's argument is that (2.10) has to be satisfied when performing a measurement both at the input and at the output of an amplifier. Based on this argument he showed that the minimum noise power contribution by a PIA is [19]

$$P_{\mathrm{N}} = \frac{\hbar\omega B_0}{2}(G_{\mathrm{PIA}} - 1) \tag{2.11}$$

where B_0 is the amplifier bandwidth and G_{PIA} is the amplifier gain. With gain $G_{\mathrm{PIA}} > 1$ the amplifier must thus add noise to the signal. If this noise was not added by the amplifier then it would be possible to gain information about the input signal, with better accuracy then stated by the uncertainty principle, by measuring the output signal. In the limit of high gain ($G_{\mathrm{PIA}} \gg 1$) (2.11) state that the noise added by the amplifier is equal to the amplification of the zero-point fluctuations present at the amplifier input.

An alternative approach for quantifying the noise added by an amplifier is to consider the in-phase and quadrature component of the signal. This approach will give both a value for the noise added by the amplifier and a lower limit for

the amplifier NF. We follow the method in [11] which treat a one-mode linear amplifier. The results below should be compared to the results obtained for a two-mode parametric amplifier in section 3.4.

In analogy with the input mode operators $\hat{X}_1$ and $\hat{X}_2$ we introduce the output mode operators $\hat{Y}_1$ and $\hat{Y}_2$. The uncertainty in the in-phase and quadrature component, $\langle\hat{Y}_1\rangle$ and $\langle\hat{Y}_2\rangle$, is given by

$$\left\langle(\Delta\hat{Y}_{\rm i})^2\right\rangle = G_{\rm i}\left\langle(\Delta\hat{X}_{\rm i})^2\right\rangle + \left\langle(\Delta\hat{F}_{\rm i})^2\right\rangle \tag{2.12}$$

where G_i denote the gain and $i \in \{1, 2\}$. The first term on the right hand side represent the amplified input noise and the second term the noise added by the amplifier. Based on this equation we can define the added noise number

$$A_{\rm i} = \frac{\left\langle\left|\Delta\hat{F}_{\rm i}\right|^2\right\rangle}{G_{\rm i}} \tag{2.13}$$

which describe the added noise referred to the amplifier input in units of number of quanta.

PIAs handle both the in-phase and quadrature component identically, since their response is insensitive to the signal phase, and therefore a single noise number A is sufficient to describe the amplifier. The noise number A satisfy the inequality [11]

$$A \geq \frac{1}{2}\left|1 - \frac{1}{G_{\rm PIA}}\right|, \tag{2.14}$$

which is expressed in units of number of quanta. (2.14) is know as the fundamental theorem for PI linear amplifiers [11]. The significance of this relation is the same as for (2.11), for high gain $G_{\rm PIA} \gg 1$ the minimum noise contribution of the amplifier is equivalent to an additional zero-point fluctuation quantity at the input.

Using (2.14), an inequality for the PIA NF can now be derived, as [11]

$${\rm NF}_{\rm PIA} \geq \left|2 - \frac{1}{G_{\rm PIA}}\right| \tag{2.15}$$

for gains $G_{\rm PIA} \geq 1$. In the limit of high gain $G_{\rm PIA} \gg 1$ we get ${\rm NF}_{\rm PIA} = 2$ (3 dB) which is the quantum limited NF for PIAs.

In figure 2.4(a) we illustrate the amplification of a state by a PIA. Characteristic for PI amplification is that noise is added, which is illustrated by the increased area, and that equal amount of noise is added to the in-phase and quadrature component, thus maintaining the circular shape of the coherent input signal.

2.2.3 Phase-sensitive amplifiers

For PIAs one noise number was enough to describe the added noise. For PSAs, whose response depend on the signal phase, two noise numbers A_1 and A_2 (and

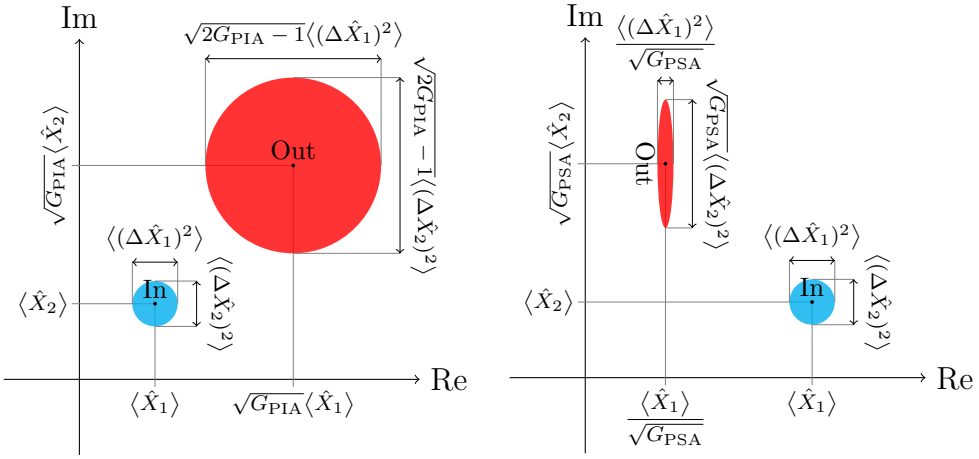

(a) PI amplification with $G_{\mathrm{PIA}} = 8$.

(b) PS amplification with $G_{\mathrm{PSA}} = 8$.

Figure 2.4: Phasor plots illustrating PI and one-mode PS amplification of an input signal (blue) yielding an output signal (red).

two gain numbers G_1 and G_2) are needed, since the in-phase and quadrature component is treated differently by the amplifier. The fundamental theorem for PIAs is replaced by the more general amplifier uncertainty principle [11]

$$A_1 A_2 \geq \frac{1}{16}\left|1 - \frac{1}{\sqrt{G_1 G_2}}\right|^2. \tag{2.16}$$

We note from (2.16) that the added noise to either the in-phase or quadrate component can be reduced at the expense of the noise added to the other component. In particular, if $G_1 = 1/G_2 = G_{\mathrm{PSA}}$, which is always the case for parametric amplifiers with signal and idler gain, then the right hand side of (2.16) vanishes and at least one component can be amplified without the addition of noise.

By analyzing the one-mode PSA in detail, in a similar manner to what will be done for two-mode PSAs in section 3.4, it can be found that both the signal and noise fields in the component amplified by G_{PSA} will experience the same gain. The consequence of this is that the amplified signal component will be amplified with a 0 dB NF. The signal and noise fields in the attenuated component will be attenuated in the corresponding manner. However, as the noise is attenuated to the level of the zero-point fluctuations then the NF will start to increase. The amplification of a state using a PSA is illustrated in figure 2.4(b).

2.3 Noise in multi-span links

Long-haul fiber optical communication systems typically consist of cascaded sections of loss, due to the optical fiber, and amplification, from lumped optical

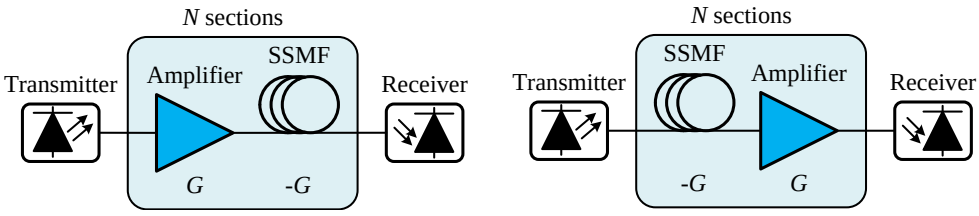

(a) Type A (b) Type B

Figure 2.5: Illustration of possible in-line amplifier configurations.

amplifiers. The noise performance of the complete system can be quantified using the so-called link NF.

We will consider two different link designs, type A and type B, illustrated in figure 2.5(a) and 2.5(b), respectively. These two systems have been extensively studied for the case of ideal PI amplification and ideal PS amplification [9, 40]. The link NF for the type A link is [41]

$$\mathrm{NF}_{\mathrm{A,PIA}} = 1 + 2N\left(1 - \frac{1}{G}\right) \quad \text{and} \quad \mathrm{NF}_{\mathrm{A,PSA}} = 1 + N\left(1 - \frac{1}{G}\right) \tag{2.17}$$

and for the type B link

$$\mathrm{NF}_{\mathrm{B,PIA}} = 1 + 2NG\left(1 - \frac{1}{G}\right) \quad \text{and} \quad \mathrm{NF}_{\mathrm{B,PSA}} = 1 + NG\left(1 - \frac{1}{G}\right) \tag{2.18}$$

where N is the number of spans and G is the amplifier gain, $-G$ is the fiber loss. From (2.17) and (2.18) it is clear that a PSA-amplified link have a 3 dB lower link NF in the case of high gain ($G \gg 1$) and many spans. A 3 dB link NF advantage could e.g. translate into doubled transmission reach which is a substantial improvement.

Chapter 3

Fiber optical parametric amplifiers

It was early realized that FOPAs have attractive properties, e.g. high gain, large bandwidth, and capability of sub-3 dB NF, when operated in PS-mode. However, due to absence of equipment, such as high-power amplifiers and high-quality optical fibers with high nonlinear coefficient, the number of experimental studies on FOPAs in general and PS-FOPAs in particular has been limited.

Advances in hardware and experimental techniques has recently opened up new possibilities to experimentally study FOPAs. These studies have confirmed that FOPAs are very capable amplifiers and signal processing platforms. Especially exciting are the demonstrations of sub-3 dB NF operation.

Chapter outline

The goal of this chapter is to give a detailed description of FOPAs. We start in section 3.1 by giving an introduction to the topic. FOPAs are based on FWM, this phenomenon is described in section 3.2. In section 3.3 we describe the gain properties of FOPAs. We introduce a transfer matrix description in section 3.4 and use that to describe the difference between PI and PS parametric amplifiers. Finally, in section 3.5 we describe how FOPAs are implemented in practice.

FOPAs, operated both in PI- and PS-mode, are a central part of the work in [Paper A-C] and thus also one of the main topics of this thesis.

3.1 Introduction

FOPAs utilize FWM, a nonlinear phenomenon, to achieve amplification. The gain mechanism is called parametric amplification or parametric gain and describe the process when energy is transferred between several interacting waves without any energy storage in the medium. One possible process is when energy is transferred

from a strong wave (pump) to a weaker wave (signal), accompanied by the generation of a third wave (idler).

Parametric amplification is a rich phenomenon and different behavior can be obtained, e.g. by varying the frequency of the interacting waves yielding different amplification schemes. Furthermore, parametric amplification can be either PI or PS. Operated in PS-mode parametric amplifiers are capable of noiseless amplification [11]. Another feature of PS operation is the possibility to generate squeezed states [42]. A squeezed state is a state in which the noise, or uncertainty, in one component (in-phase or quadrature) is reduced at the expense of the noise in the other component.

The interaction between an electromagnetic wave and the medium it propagate through is governed by the material susceptibility χ [43, p. 15]. At high field intensities not only the linear susceptibility will be of importance but also higher order susceptibilities, which result in a nonlinear response. In materials without inversion symmetry, such as many crystals, the 2nd-order susceptibility $\chi^{(2)}$ will be the dominating higher order susceptibility and give rise to e.g. second harmonic generation (SHG) and sum-frequency generation. In isotropic materials, such as silica (SiO_2) glass, all even-order susceptibilities vanishes and the 3rd-order susceptibility $\chi^{(3)}$ will dominate.

Parametric amplification can be obtained both in $\chi^{(2)}$ materials [44–47], and $\chi^{(3)}$ materials [48, 49]. It is in many cases preferable to work with fiber-based amplifiers due to compatibility with fiber optical transmission systems. In optical fibers, which are made of silica glass, $\chi^{(3)}$ dominate and will give rise to FWM, which can provide parametric gain. These devices are called FOPAs.

FOPAs can be operated both using pulsed and continuous wave (CW) pumps. The first FOPAs were demonstrated with pulsed pumps [48,50,51]. Using a pulsed pump, with high peak power, eases the requirements on the other parts of the system and high gain can be obtained over short lengths of fiber with only modest nonlinear coefficient. However, for most communication related applications a CW pump is required.

In order to demonstrate FOPAs with CW pumps, fibers with high nonlinear coefficient and low zero-dispersion wavelength (ZDW) variations are required. Furthermore, a high-power pump source is needed. These requirements slowed the development of FOPAs for a long time and it was not until the mid-1990's that progress started to gain pace and CW pumped FOPAs were demonstrated [52]. Particularly noteworthy is the first demonstration of a CW pumped FOPA with significant black-box gain [53].

The gain mechanism in FOPAs is fundamentally different from the mechanism that provide gain in EDFAs, which also lead to fundamentally different amplifier properties. The operating range and bandwidth of FOPAs is mainly determined by the system design. FOPAs have been demonstrated with gain over a large range of frequencies and with bandwidths as large as 81 nm using a dual-pumped configuration [54]. Gain values of 70 dB have been demonstrated [14], and the

gain efficiency is comparable to that of Raman amplifiers with $\sim$ 10 mW pump power per dB gain. A NF of 3.7 dB has been demonstrated for phase-insensitive fiber optical parametric amplifiers (PI-FOPAs) [55], and 1.1 dB at 26.5 dB gain for PS-FOPAs [56].

A basic property of parametric amplifiers is the ultra-fast gain mechanism with a femtosecond response time. This should be compared to the millisecond response time in EDFAs. While this prevent FOPAs from operating in saturation it opens up for nonlinear signal processing applications. Some demonstrations of nonlinear signal processing using parametric effects in fibers are sampling [57], demultiplexing [58], amplitude regeneration [59], and format conversion [60].

Another property that is fundamentally connected to the gain mechanism is the polarization dependence of the gain. This is a major drawback for transmission system applications. However, at the expense of efficiency, it is possible to obtain polarization insensitive operation using two orthogonally polarized pumps [61,62].

3.2 Four-wave mixing

FWM, also named four-photon mixing, originates from the $\chi^{(3)}$ nonlinearity and involves the interaction of four waves. An intuitive understanding of the process can be obtained by considering the refractive index modulation that is induced by a high intensity wave through the Kerr-effect.

If two waves at frequencies ω_1 and ω_2 co-propagate through a fiber then they will beat at a frequency $\omega_2 - \omega_1$ and through this intensity beating modulate the refractive index with the same frequency. If a third wave is added, with frequency ω_3, then it will become phase modulated with the frequency $\omega_2 - \omega_1$ and develop sidebands at $\omega_3 \pm (\omega_2 - \omega_1)$ due to the modulated refractive index. Similarly will ω_3 beat with ω_1 and phase modulate ω_2 such that ω_2 generate sidebands at $\omega_2 \pm (\omega_3 - \omega_1)$. Considering all possible combinations, new frequency components will be generated at $\omega_{\mathrm{jkl}} = \omega_{\mathrm{j}} + \omega_{\mathrm{k}} - \omega_{\mathrm{l}}$ with $\mathrm{j,k,l} \in \{1,2,3\}$ [63]. Some of these components will overlap, either with each other or with the original waves. Components that overlap with the original waves provide gain. There will be nine newly generated frequency components and these will have varying power, the stronger ones are usually referred to as idlers and the weaker ones are usually neglected.

For the specific case of one degenerate strong wave (pump) and one weaker wave (signal) one significant new frequency component will be generated (idler) and gain will be provided to the signal. This is the case we are dealing with in this thesis, called single (degenerate) pump nondegenerate idler scheme. The FWM process is highly polarization dependent and in the discussion we will assume that all waves have the same state of polarization over the entire interaction length.

In a quantum mechanical picture FWM can be understood as the annihilation of two photons and the creation of two photons, with frequencies such that

momentum and energy is conserved. In the case of degenerate FWM, where two waves have the same frequency ω_1, the process must satisfy $2\omega_1 = \omega_2 + \omega_3$ and $\Delta\beta = \beta_2 + \beta_3 - 2\beta_1 = 0$.

To get a more complete description of FWM we consider the electromagnetic fields of three co-polarized waves propagating in a standard single mode fiber (SSMF). One degenerate pump wave, denoted by index p, one signal wave, denoted by index s, and an idler wave, denoted by index i. The sum of the electrical fields can be written as [43]

$$E(x,y,z) = \frac{f(x,y)}{2} \sum_{k\in\{\mathrm{p,s,i}\}} \Big\{ A_k(z) \exp\left[i(\beta_k z - \omega_k t)\right] \Big\} + \text{c.c.} \tag{3.1}$$

where c.c. denote the complex conjugate which is usually omitted in the calculations and $f(x,y)$ is the transverse mode profile, common for all waves. Each of the three waves is represented by the slowly varying complex field amplitude $A(z)$, the propagation constant β, and the frequency ω. By inserting (3.1) into the nonlinear Schrödinger equation (NLSE) the following coupled equations can be derived [43]

$$\frac{dA_\mathrm{p}}{dz} = i\gamma \left\{ \left[|A_\mathrm{p}|^2 + 2\Big(|A_\mathrm{s}|^2 + |A_\mathrm{i}|^2 \Big) \right] A_\mathrm{p} + 2A_\mathrm{s}A_\mathrm{i}A_\mathrm{p}^* \exp\left(i\Delta\beta z\right) \right\}, \tag{3.2}$$

$$\frac{dA_\mathrm{s}}{dz} = i\gamma \left\{ \left[|A_\mathrm{s}|^2 + 2\Big(|A_\mathrm{p}|^2 + |A_\mathrm{i}|^2 \Big) \right] A_\mathrm{s} + A_\mathrm{i}^* A_\mathrm{p}^2 \exp\left(-i\Delta\beta z\right) \right\}, \tag{3.3}$$

$$\frac{dA_\mathrm{i}}{dz} = i\gamma \left\{ \left[|A_\mathrm{i}|^2 + 2\Big(|A_\mathrm{p}|^2 + |A_\mathrm{s}|^2 \Big) \right] A_\mathrm{i} + A_\mathrm{s}^* A_\mathrm{p}^2 \exp\left(-i\Delta\beta z\right) \right\}, \tag{3.4}$$

where

$$\Delta\beta = 2\beta_\mathrm{p} - \beta_\mathrm{s} - \beta_\mathrm{i} \tag{3.5}$$

is the propagation constant mismatch and γ is the nonlinear coefficient. In order to arrive at this set of equations we have neglected fiber attenuation, higher-order dispersion, any wavelength dependence of γ, and the Raman effect.

We note that the first two terms on the right hand side of (3.2)-(3.4) give rise to a nonlinear phase-shift, the first term corresponds to SPM and the second to XPM. The last term governs a power transfer between the waves and is due to FWM. It is clear that the FWM term is dependent on $\Delta\beta$, which is determined by the relative phase of the waves. We also note that XPM and SPM do not need phase-matching since they only depend on the intensity.

By defining $A_\mathrm{j} = \sqrt{P_\mathrm{j}}\exp(i\phi_\mathrm{j})$ for $\mathrm{j} \in \{\mathrm{p,s,i}\}$ where P_j is the power and ϕ_j is the phase of wave j, (3.2)-(3.5) can be written as [15]

$$\frac{dP_\mathrm{p}}{dz} = -4\gamma (P_\mathrm{p}^2 P_\mathrm{s} P_\mathrm{i})^{1/2} \sin(\theta), \tag{3.6}$$

$$\frac{dP_\mathrm{s}}{dz} = \frac{dP_\mathrm{i}}{dz} = 2\gamma(P_\mathrm{p}^2 P_\mathrm{s} P_\mathrm{i})^{1/2}\sin(\theta), \tag{3.7}$$

and

$$\frac{d\theta}{dz} = \Delta\beta + \gamma(2P_\mathrm{p} - P_\mathrm{s} - P_\mathrm{i}) + \left(\sqrt{\frac{P_\mathrm{p}^2 P_\mathrm{s}}{P_\mathrm{i}}} + \sqrt{\frac{P_\mathrm{p}^2 P_\mathrm{i}}{P_\mathrm{s}}} - 4\sqrt{P_\mathrm{s}P_\mathrm{i}}\right)\cos(\theta) \tag{3.8}$$

where $\theta = 2\phi_\mathrm{p} - \phi_\mathrm{s} - \phi_\mathrm{i}$. It is clear from (3.6) and (3.7) that the FWM efficiency is maximized for $\theta = \pi/2$. This condition is referred to as the process being phase-matched. If $\theta = \pi/2$ then the last term in (3.8) will be zero and in order for the process to stay phase-matched we need

$$\kappa = \Delta\beta + 2\gamma P_\mathrm{p} = 0, \tag{3.9}$$

assuming that the pump power is much larger than signal and idler powers.

Before we move on to discuss the phase-matching condition in more detail we note from (3.6) and (3.7) that the direction in which the energy is transferred, from the pump to the signal and idler or from the signal and idler to the pump, depends on the relative phase θ. For the parametric gain process to be efficient it is thus important that the relative phase is kept constant throughout the interaction length.

3.2.1 Phase-matching

Phase-matching refers to keeping the relative phase θ of the interacting waves constant during propagation, and is essential in order to obtain high FWM efficiency. The interacting waves will acquire a phase-shift during propagation due to linear and nonlinear effects. This is illustrated by (3.9), where the first term on the right hand side represent the linear phase-shift, which is induced by the difference in propagation constant between the waves, and the second term represent the nonlinear phase-shift which is due to SPM and XPM. In practice phase-matching means making sure the linear and nonlinear phase-shifts cancel out, also referred to as nonlinear phase-matching, and the relative phase θ kept constant.

We see from (3.9) that in order for phase-matching to be feasible $\Delta\beta$ must be negative. In the single (degenerate) pump case with the pump frequency ω_p close to the fiber zero dispersion frequency ω_0 the phase-matching condition can be written as [15]

$$\kappa = \beta_3(\omega_\mathrm{p} - \omega_0)(\omega_\mathrm{s} - \omega_\mathrm{p})^2 + 2\gamma P_\mathrm{p} = 0 \tag{3.10}$$

where β_3 is the third derivative of the propagation constant at ω_0. From (3.10) we see that phase-matching is only possible if the pump is in the anomalous dispersion regime, which is important to consider when designing a FOPA. From (3.10) we can also see that there are only two signal frequencies that give $\kappa = 0$. There will thus be two gain maxima, one on either side of the pump. Furthermore, we

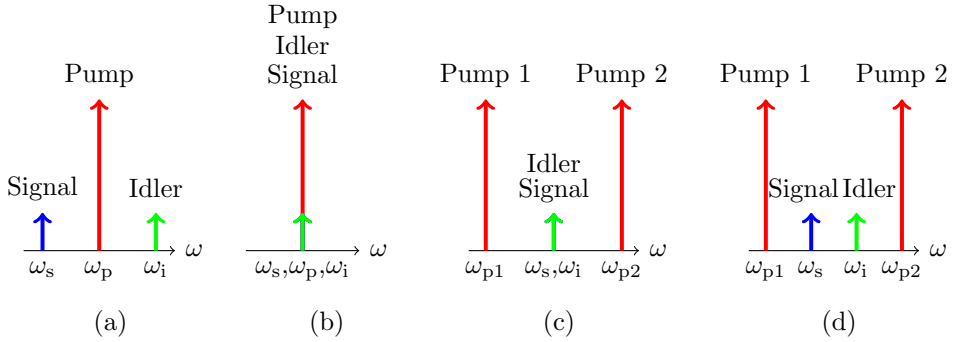

Figure 3.1: Illustration of single pump (a) nondegenerate idler and (b) degenerate idler and dual pump (c) degenerate idler and (d) nondegenerate idler schemes.

note that gain bandwidth will increase with decreased dispersion slope, due to a reduced dependence on the frequency selection of the waves.

In the case when no idler wave is present at the input then an idler will be generated in the FOPA and take a phase such that the relative phase θ is $\pi/2$. In that case the gain is independent of the signal phase at the input and the amplifier is said to be phase-insensitive. On the other hand when the idler is present at the input then the gain will be dependent on the signal phase and the amplifier is phase-sensitive.

3.3 Parametric amplification

Based on the previous section we can think of parametric amplification in $\chi^{(3)}$ media as phase-matched FWM where one or two pump waves transfer energy to a weak signal wave. Depending of how the wavelengths are selected different schemes, with different properties, can be obtained.

A single (degenerate) pump case can be either degenerate or nondegenerate idler type, depending on how the signal frequency is chosen. According to conservation of energy, the waves should satisfy the relation $2\omega_p = \omega_s + \omega_i$. This can be done either by positioning the signal on the side of the pump or at the same frequency as the pump. In the dual (nondegenerate) pump case the waves must satisfy the relation $\omega_{p1} + \omega_{p2} = \omega_s + \omega_i$. In this case we can also have either a degenerate idler or nondegenerate idler scheme. The different schemes are illustrated in figure 3.1.

The degenerate idler case is also commonly called one-mode and will automatically be PS. The nondegenerate idler case, also called two-mode, will be PS if an idler wave at the correct frequency is present at the input. If the idler wave is not present then it will be generated internally, at the wavelength given by energy conservation, and the process is PI.

For the purpose of amplification we are interested in the amplifier gain. An expression for the gain can be derived from (3.2)-(3.4). We assume that the pump wave(s) are much stronger than the signal and idler waves during the whole process, i.e. there is no pump depletion. In this case one might set $dA_{\mathrm{p}}/dz = 0$ and the signal gain G is given by [15]

$$G = \left\{ 1 + \left[\frac{\gamma P_{\mathrm{p}}}{g} \sinh(g L_{\mathrm{eff}}) \right] \right\}^2 \tag{3.11}$$

where g is the parametric gain coefficient given by

$$g = \left[(\gamma P_{\mathrm{p}})^2 - \left(\frac{\kappa}{2} \right)^2 \right] \tag{3.12}$$

and L_{eff} is the effective length defined by $L_{\mathrm{eff}} = \big[1 - \exp(-\alpha L)\big]/\alpha$, with α denoting the fiber loss coefficient and L the fiber length.

We remind ourselves that κ describe the phase-matching and in the case of perfect nonlinear phase-matching, i.e. when $\kappa = 0$, and $\gamma P_{\mathrm{p}} L_{\mathrm{eff}} \gg 1$ then the expression for the signal gain simplifies to [15]

$$G \approx \frac{1}{4} \exp(2\gamma P_{\mathrm{p}} L_{\mathrm{eff}}). \tag{3.13}$$

We note from (3.13) that in this case the signal will grow exponentially with respect to pump power, this is called the exponential gain regime.

Another interesting regime is when there is no relative phase-shift due to dispersion, i.e. when the signal and pump are at the same wavelength, and consequently $\kappa = -2\gamma P_{\mathrm{p}}$. In this case the signal gain simplifies to [15]

$$G \approx (2\gamma P_{\mathrm{p}} L_{\mathrm{eff}})^2 \tag{3.14}$$

and we note the quadratic dependence on the pump power. This regime is called the quadratic gain regime.

It is important to realize that FWM will also take place between the pump(s) and the zero-point fluctuations that are always present at all frequencies. This will give rise to amplified quantum noise (AQN), also called parametric ASE.

3.4 Transfer matrix description

Using a transfer matrix to describe a system is common in a number of fields. The method is particularly convenient when analyzing cascaded systems, in which case a transfer matrix for the combined system is obtained simply by multiplying the transfer matrices of the individual sub-systems. A general system with two input

ports and two output ports can be described by

$$\begin{bmatrix} B_1 \\ B_2 \end{bmatrix} = \underbrace{\begin{bmatrix} s_{11} & s_{12} \\ s_{21} & s_{22} \end{bmatrix}}_{\mathbf{S}} \begin{bmatrix} A_1 \\ A_2 \end{bmatrix} \tag{3.15}$$

where A_1 and A_2 are the input modes, B_1 and B_2 are the output modes and $\mathbf{S}$ is the transfer matrix.

In optics the modes can be represented by the complex amplitude, which contain information both about the amplitude and the phase. Transfer matrices can be used to describe e.g. beam splitters and combiners, optical couplers, and parametric processes.

A general two-mode parametric process with signal and idler gain can, when the pump wave(s) are treated as constant fields (no pump depletion), be described by [64]

$$\begin{bmatrix} B_\mathrm{s} \\ B_\mathrm{i}^* \end{bmatrix} = \begin{bmatrix} \mu & \nu \\ \nu^* & \mu^* \end{bmatrix} \begin{bmatrix} A_\mathrm{s} \\ A_\mathrm{i}^* \end{bmatrix} \tag{3.16}$$

where index s and i denote the signal and idler waves respectively, superscript $*$ represent the complex conjugate, and μ and ν are complex transfer coefficients. The exact form of μ and ν can be found in [65], but are not important for the analysis presented here. We will be contented by knowing that they depend on the pump power, the phase-matching, the nonlinear interaction strength and the polarization state. However, it is important that μ and ν satisfy the relation [64]

$$|\mu|^2 - |\nu|^2 = 1 \tag{3.17}$$

which in practice mean that the signal and idler waves experience gain and are amplified.

To gain insight about the parametric process we evaluate (3.16) and get the transfer function

$$\begin{cases} B_\mathrm{s} = \mu A_\mathrm{s} + \nu A_\mathrm{i}^* \\ B_\mathrm{i} = \nu A_\mathrm{s}^* + \mu A_\mathrm{i}. \end{cases} \tag{3.18}$$

Due to the coupled propagation of the signal and idler waves it is not easy to interpret (3.18). However, the two coupled propagation equations (3.18) can be written as two independent modes by carrying out the variable substitution

$$\begin{cases} A_+ = \dfrac{A_\mathrm{s} + A_\mathrm{i}}{\sqrt{2}} \\ A_- = \dfrac{A_\mathrm{s} - A_\mathrm{i}}{\sqrt{2}} \end{cases} \tag{3.19}$$

which gives us, see A.1,

$$\begin{cases} B_+ = \mu A_+ + \nu A_+^* \\ B_- = \mu A_- - \nu A_-^* \end{cases} \tag{3.20}$$

where B_+ and B_- are defined analogous to A_+ and A_-. We take one more step and rewrite this set of equations, see A.2, and end up with

$$\begin{cases} B_+ = \exp(i\theta_{\mathrm{r}}^+)\Big[\big(|\mu| + |\nu|\big)\mathrm{Re}(A_{\mathrm{r},+}) + i\big(|\mu| - |\nu|\big)\mathrm{Im}(A_{\mathrm{r},+})\Big] \\ B_- = \exp(i\theta_{\mathrm{r}}^+)\Big[\big(|\mu| - |\nu|\big)\mathrm{Re}(A_{\mathrm{r},-}) + i\big(|\mu| + |\nu|\big)\mathrm{Im}(A_{\mathrm{r},-})\Big] \end{cases} \tag{3.21}$$

where

$$A_{\mathrm{r},+} = A_+ \exp(i\theta_{\mathrm{r}}^-) \quad \text{and} \quad A_{\mathrm{r},-} = A_- \exp(i\theta_{\mathrm{r}}^-) \tag{3.22}$$

and

$$\theta_{\mathrm{r}}^+ = \frac{\theta_\mu + \theta_\nu}{2} \quad \text{and} \quad \theta_{\mathrm{r}}^- = \frac{\theta_\mu - \theta_\nu}{2}. \tag{3.23}$$

The angles θ_μ and θ_ν are defined by $\mu = |\mu|\exp(i\theta_\mu)$ and $\nu = |\nu|\exp(i\theta_\nu)$, respectively. From (3.21) we see that one component of each mode, either in-phase or quadrature, will be amplified by $G = (|\mu| + |\nu|)^2$ while the other component will be attenuated by $1/G = (|\mu| - |\nu|)^2$. This is an important conclusion since it tells us that a two wave (mode) parametric amplifier can phase-sensitively amplify two independent components. The relation $(|\mu| + |\nu|)^2 = 1/(|\mu| - |\nu|)^2$ can be shown using $|\mu|^2 - |\nu|^2 = 1$.

Up until this point we have not considered the quantum noise in our models of the FOPA. In the transfer matrix description quantum noise can easily be included by adding a noise term n to the input modes

$$\begin{bmatrix} B_{\mathrm{s}} \\ B_{\mathrm{i}}^* \end{bmatrix} = \begin{bmatrix} \mu & \nu \\ \nu^* & \mu^* \end{bmatrix} \begin{bmatrix} A_{\mathrm{s}} + n_{\mathrm{s}} \\ A_{\mathrm{i}}^* + n_{\mathrm{i}}^* \end{bmatrix} \tag{3.24}$$

where n_{s} and n_{i} is the quantum noise associated with the signal and idler waves, respectively. The noise is taken as additive Gaussian noise that satisfies $\langle n_m \rangle = 0$, $\langle n_m n_l \rangle = 0$, and $\langle |n_m|^2 \rangle = \hbar\omega_m/2$ with $m, l \in \{\mathrm{s}, \mathrm{i}\}$ [64]. The model given by (3.24), with the assumption of Gaussian noise at the input, is a so-called semiclassical model.

By evaluating 3.24 we get the transfer function

$$\begin{cases} B_{\mathrm{s}} = \mu A_{\mathrm{s}} + \nu A_{\mathrm{i}}^* + \mu n_{\mathrm{s}} + \nu n_{\mathrm{i}}^* \\ B_{\mathrm{i}} = \nu A_{\mathrm{s}}^* + \mu A_{\mathrm{i}} + \nu n_{\mathrm{s}}^* + \mu n_{\mathrm{i}}. \end{cases} \tag{3.25}$$

Given that the noise, n_{s} and n_{i}, are uncorrelated vacuum fluctuations then the noise gain through the parametric amplifier will be $|\mu|^2 + |\nu|^2$, independent of the

signal and idler modes. As we will see below, the gain in PI-mode $G_{\mathrm{PIA}} = |\mu|^2$ and thus the noise gain can be written as $|\mu|^2 + |\nu|^2 = 2|\mu|^2 - 1 = 2G_{\mathrm{PIA}} - 1$. From (3.25) we see that the noise at the output of the parametric amplifier will be correlated. This will be of importance when studying the so-called copier-PSA scheme, used to realize PSA-amplified links, in which two parametric amplifiers are cascaded.

The model given by (3.24) is a semiclassical description of a quantum mechanical system. However, it has been proved that the results given by the semiclassical model are of comparable accuracy with those from a complete quantum mechanical model, given that the photon-number is large [17, 66].

In the following sections we will analyze three cases in more detail. First the case of PI amplification and then the case of degenerate and nondegenerate idler PS amplification.

3.4.1 Phase-insensitive mode

In PI-mode no idler wave is present at the input, i.e. $A_{\mathrm{i}} = 0$, and the general input-output relation (3.16) take the form

$$\begin{bmatrix} B_{\mathrm{s}} \\ B_{\mathrm{i}}^* \end{bmatrix} = \begin{bmatrix} \mu & \nu \\ \nu^* & \mu^* \end{bmatrix} \begin{bmatrix} A_{\mathrm{s}} \\ 0 \end{bmatrix}. \tag{3.26}$$

By evaluating (3.26) we obtain the transfer function

$$\begin{cases} B_{\mathrm{s}} = \mu A_{\mathrm{s}} \\ B_{\mathrm{i}} = \nu A_{\mathrm{s}}^* \end{cases} \tag{3.27}$$

and we see that the output signal will be the input signal amplified by $G_{\mathrm{PIA}} = |\mu|^2$ and the output idler will be a phase-conjugated copy of the signal amplified by $|\nu|^2 = G_{\mathrm{PIA}} - 1$, given that θ_μ and θ_ν are both zero.

Based on the previous calculation of the noise gain we can now calculate the PIA NF for the signal

$$\mathrm{NF}_{\mathrm{PIA}} = \frac{2G_{\mathrm{PIA}} - 1}{G_{\mathrm{PIA}}} = 2 - \frac{1}{G_{\mathrm{PIA}}} \tag{3.28}$$

which in the limit of high gain ($G_{\mathrm{PIA}} \gg 1$) take the value 2 (3 dB). The input and output modes of a PI parametric amplifier, with $\theta_\mu = \theta_\nu = 0$ and $G_{\mathrm{PIA}} = 8$, are illustrated in figure 3.2(a).

3.4.2 Phase-sensitive mode

PS-mode is obtained when an idler wave is present at the input, i.e. $A_{\mathrm{i}} \neq 0$. We will consider two illustrative cases that will help us to understand the workings of PSAs.

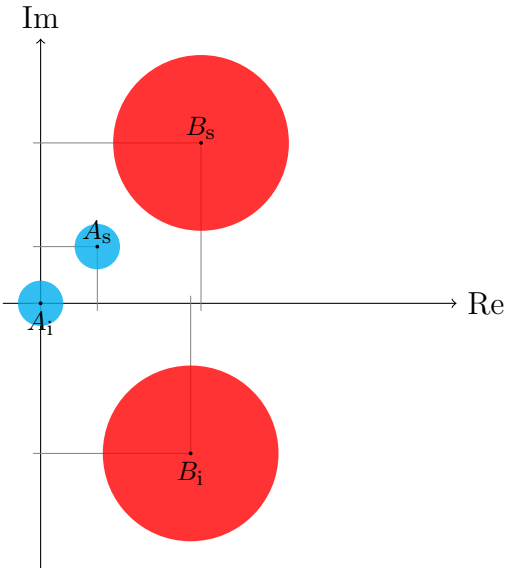

(a) PI mode ($A_\mathrm{i} = 0$)

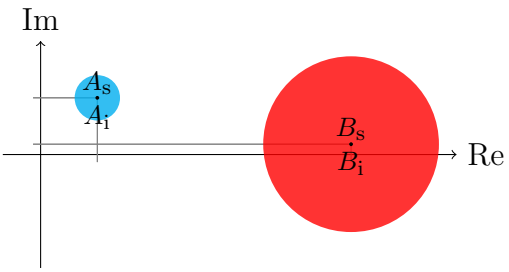

(b) PS mode with $A_\mathrm{i} = A_\mathrm{s}$

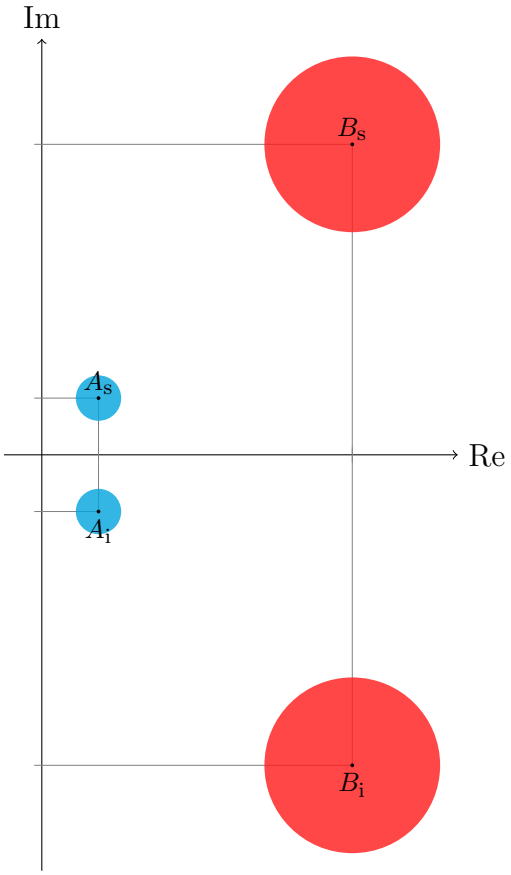

(c) PS mode with $A_\mathrm{i} = A_\mathrm{s}^*$

Figure 3.2: Illustration of input (blue) and output (red) modes for parametric amplification with the angles $\theta_\mu = \theta_\nu = 0$ and $G_\mathrm{PIA} = 8$. In all cases the noise gain is $2G_\mathrm{PIA} - 1$ while the signal and idler gain varies.

Phase-sensitive mode case: $A_{\mathrm{i}} = A_{\mathrm{s}}$

We first consider the case when the idler wave is an exact copy of the signal, i.e. $A_{\mathrm{i}} = A_{\mathrm{s}}$. The general input-output relation (3.16) take the form

$$\begin{bmatrix} B_{\mathrm{s}} \\ B_{\mathrm{i}}^* \end{bmatrix} = \begin{bmatrix} \mu & \nu \\ \nu^* & \mu^* \end{bmatrix} \begin{bmatrix} A_{\mathrm{s}} \\ A_{\mathrm{s}}^* \end{bmatrix} \tag{3.29}$$

and by evaluating this relation we get the transfer function

$$\begin{cases} B_{\mathrm{s}} = \mu A_{\mathrm{s}} + \nu A_{\mathrm{s}}^* \\ \\ B_{\mathrm{i}} = \mu A_{\mathrm{s}} + \nu A_{\mathrm{s}}^*. \end{cases} \tag{3.30}$$

We can immediately see from (3.30) that the output signal and idler will be identical. Evaluating (3.22) we find that

$$A_{\mathrm{r},+} = \sqrt{2} A_{\mathrm{s}} \exp(i\theta_{\mathrm{r}}^-) \quad \text{and} \quad A_{\mathrm{r},-} = 0. \tag{3.31}$$

Since one of the modes is zero we can conclude that only one signal component, either in-phase or quadrature, will be amplified by $G_{\mathrm{PSA}} = (|\mu|+|\nu|)^2 = (\sqrt{G_{\mathrm{PIA}}}+\sqrt{G_{\mathrm{PIA}}-1})^2$ while the other component will be attenuated by $1/G_{\mathrm{PSA}}$. We note that in the limit of high gain, i.e. $|\mu| \approx |\nu|$, then $G_{\mathrm{PSA}} = 4G_{\mathrm{PIA}}$, or in other words the PSA gain is 6 dB higher than the PIA gain. This gain advantage is explained by the coherent addition of the signal and idler fields.

In the same was as we calculated the signal NF for the PIA we can calculate the signal NF for the PSA. However, since one signal component will be amplified and the other component attenuated we will obtain two NFs. For the amplified component we get

$$\mathrm{NF}_{\mathrm{PSA,amp}} = \frac{2G_{\mathrm{PIA}} - 1}{\left(\sqrt{G_{\mathrm{PIA}}} + \sqrt{G_{\mathrm{PIA}} - 1}\right)^2} \longrightarrow \frac{1}{2}, \tag{3.32}$$

and for the attenuated component we get

$$\mathrm{NF}_{\mathrm{PSA,att}} = \frac{2G_{\mathrm{PIA}} - 1}{\left(\sqrt{G_{\mathrm{PIA}}} - \sqrt{G_{\mathrm{PIA}} - 1}\right)^2} \longrightarrow 8G_{\mathrm{PIA}}^2 \tag{3.33}$$

where the limits are taken for $G_{\mathrm{PIA}} \to \infty$. The negative NF of -3 dB (1/2) for the amplified component might seem confusing but find its explanation in the strong nonlinear coupling between signal and idler modes at high gain. In (3.33) only the signal input power is considered but due to the coupling also the idler power should be taken into account which increase the input SNR by 3 dB and thus result in a NF of 0 dB. In figure 3.2(b) we illustrate the input and output modes of a degenerate idler PS parametric amplifier for the case when $\theta_\mu = \theta_\nu = 0$ and $G_{\mathrm{PIA}} = 8$.

Phase-sensitive mode case: $A_\mathrm{i} = A_\mathrm{s}^*$

The second case we consider is when the idler wave is a phase-conjugated copy of the signal wave, i.e. $A_\mathrm{i} = A_\mathrm{s}^*$, in which case (3.16) take the form

$$\begin{bmatrix} B_\mathrm{s} \\ B_\mathrm{i}^* \end{bmatrix} = \begin{bmatrix} \mu & \nu \\ \nu^* & \mu^* \end{bmatrix} \begin{bmatrix} A_\mathrm{s} \\ A_\mathrm{s} \end{bmatrix} \tag{3.34}$$

and by evaluating this relation we get the transfer function

$$\begin{cases} B_\mathrm{s} = \mu A_\mathrm{s} + \nu A_\mathrm{s} \\ B_\mathrm{i} = \mu A_\mathrm{s}^* + \nu A_\mathrm{s}^*. \end{cases} \tag{3.35}$$

In this case (3.22) give us

$$A_{\mathrm{r},+} = \sqrt{2}\mathrm{Re}(A_\mathrm{s}) \exp(i\theta_\mathrm{r}^-) \quad \text{and} \quad A_{\mathrm{r},-} = i\sqrt{2}\mathrm{Im}(A_\mathrm{s}) \exp(i\theta_\mathrm{r}^-), \tag{3.36}$$

which tells us that both signal components will be amplified with a gain of $G_\mathrm{PSA} = (|\mu| + |\nu|)^2$. In this case the NF for both signal components is given by $\mathrm{NF}_\mathrm{PSA,amp}$ and take the value -3 dB at high gain, or considering the idler power at the input, 0 dB. The input and output modes, with $\theta_\mu = \theta_\nu = 0$ and $G_\mathrm{PIA} = 8$, are illustrated in figure 3.2(c).

3.5 Design and implementation

The most important component in a FOPA is the optical fiber where FWM takes place. For high efficiency operation the fiber should have high nonlinear coefficient γ, ZDW in the anomalous regime, in or close to the C-band, and low dispersion slope. Today so-called highly nonlinear fibers (HNLFs) are often used to realize FOPAs. Silica-based HNLFs can have a large nonlinear coefficient, about 20 $(\mathrm{W\ km})^{-1}$ [67]. This should be compared to the nonlinear coefficient in ordinary SSMF which is about 1.5 $(\mathrm{W\ km})^{-1}$.

Although fibers with high nonlinear coefficient are available, high pump powers and long fiber sections are still needed to obtain high gain. Fibers used for FOPAs are usually in the range of 100-1000 m and EDFAs are used to reach CW pump powers in the range of 0.5-10 W.

The amount of pump power that is launched into the HNLF, and thus also the FOPA gain, is limited by stimulated Brillouin scattering (SBS). SBS is similar to SRS in that pump power is absorbed by the material and then emitted as a frequency-shifted wave. In silica fibers the wave is down-shifted around 10 GHz and have a bandwidth of tens of MHz. The generated wave propagates in the backward direction, relative to the pump, and above a certain threshold power all

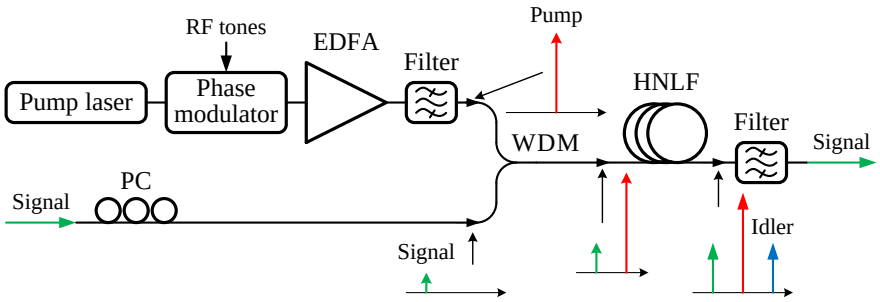

Figure 3.3: Typical implementation of a PI-FOPA with phase-modulated pump for SBS suppression. PC: polarization controller.

additional pump power will be transferred to the down-shifted wave, thus limiting the pump power.

Several methods for reducing SBS have been proposed. The most common method is to broaden the pump spectrum using a phase modulator [68]. Another technique is to concatenate several pieces of HNLF with isolators in between, in order to block and prevent the SBS to build up [69]. There are also techniques that rely on frequency-shifting the backscattered wave along the fiber, either using a temperature gradient or fiber stretching, and techniques that rely on doping the fiber, e.g. with Al or Ge.

A typical setup for a PI-FOPA using a CW pump is illustrated in figure 3.3. The pump wave originate from a laser and is then phase-modulated to reduce the SBS in the HNLF. After phase modulation the pump is boosted with an EDFA and filtered to remove ASE using a band-pass filter. The pump is then combined with the signal using a WDM coupler, in order minimize the coupling loss. Since the FWM process is polarization dependent the signal polarization has to be tuned for highest gain. After the HNLF the signal wave is filtered out.

Chapter 4

Phase-sensitively amplified links

It was early established that successful implementation of PSAs in transmission links would lead to a considerable performance improvement compared to when using PIAs. However, due to practical difficulties the first WDM compatible PSA-amplified link demonstration was published only recently.

The enabling technique for WDM compatible PSA-amplified links was the so-called copier-PSA scheme. In this scheme a PI parametric amplifier precede the PSA and generate the set of frequency- and phase-locked waves required for PS amplification. The possible amplifier configurations that can be implemented based on the copier-PSA scheme, with improved noise performance over conventional PIAs, is limited to preamplifiers and inline amplifiers.

Apart from the predicted noise improvement a nonlinear penalty reduction can also be observed when operating a PSA-amplified link in the nonlinear transmission region. However, the implementation of PSA-amplified links is challenging and the noise and nonlinear penalty mitigation benefits comes at the cost of complexity.

Chapter outline

The topic of this chapter is partially covered in [Paper A-C] and some parts will therefore be treated in less detail here. In section 4.1 we introduce the topic of PSA-amplified links and describe the historical development of the field. The possibilities and limitations of the copier-PSA scheme are described in section 4.2. In section 4.3 we briefly account for the possibility of nonlinear distortion mitigation in PSA-amplified links. Finally, in section 4.4 we give an overview of the practical challenges with implementing PSA-amplified links based on the copier-PSA scheme.

4.1 Introduction

Not long after it was realized that PSAs in theory are capable of noiseless amplification [11], the possibility of implementing PSAs in long-haul communication systems was theoretically investigated [40,70]. Most of the early experimental work on PSAs was done using one-mode PSAs [71–73]. The reason for this was that one-mode PSAs are comparably easy to implement, only requiring phase-locking of the pump wave(s) and the signal wave. However one-mode PSAs have some significant drawbacks.

For transmission applications it is in general desirable to have a PSA implementation that, apart from providing noiseless amplification, is WDM compatible and modulation format independent. One-mode PSAs are neither WDM compatible nor modulation format independent. Two-mode PSAs on the other hand are both WDM compatible and capable of modulation format independent operation. It should also be mentioned that one-mode PSAs are difficult to implement with high gain due to the quadratic dependence of the gain on the pump power [15], while two-mode PSAs and capable of providing high gain, growing exponentially with pump power [74].

A practical difficulty with two-mode PSAs is to generate the set of frequency- and phase-locked waves, often widely spaced in frequency, that is required at the input. In a pioneering study on two-mode parametric interaction three phase-locked waves were generated using an acousto-optic modulator (AOM) and PS amplification and attenuation was observed [75]. However, using an AOM to generate the waves is not a viable solution for transmission applications.

Due to a lack of schemes capable of generating phase-locked waves the experimental research on two-mode PSAs stagnated and it took almost 20 years from the first demonstration of a two-mode PSA [75], to the first demonstration of a two-mode PSA-amplified transmission link [76]. In the demonstration the frequency- and phase-locking of the waves was accomplished using an optical double-sideband modulation scheme [77, 78], and single-channel 2.5 Gbit/s non-return-to-zero (NRZ) data transmission over a 60 km dispersion compensated link was accomplished.

A drawback of the optical double-sideband modulation scheme is that the bandwidth is severely limited by the bandwidth of the optical modulators used to generate the sidebands. Frequency- and phase-locked waves can also be generated using a PI parametric amplifier. In this case the bandwidth is determined by the bandwidth of the parametric amplifier, and can therefore be very large. The combination of a PI parametric amplifier, for generating frequency- and phase-locked waves, followed by a PSA was first introduced in [16]. The scheme is commonly referred to as the copier-PSA scheme. An important feature of this scheme is that it can provide modulation format independent operation.

The first reported PSA demonstration utilizing the copier-PSA scheme showed PS amplification of three WDM channels [79,80]. However, the demonstration was

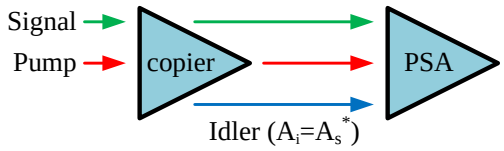

Figure 4.1: Conceptual illustration of the copier-PSA scheme.

mere a proof of concept of the WDM compatibility of the copier-PSA scheme and no data was transmitted and no transmission fiber of significant length was used in the demonstration. The first demonstration of a PSA-amplified transmission link, over a significant span of fiber, with WDM capability and modulation format independence was presented in [Paper B]. The experimental setup used for this demonstration was based on the copier-PSA scheme.

All demonstrations of two-mode PSA-amplified links to date have used a PSA operating as preamplifier. There have thus not been any demonstrations of multi-span inline two-mode PSA-amplified transmission links. However, multi-span inline PSA-amplified links have been demonstrated using one-mode PSAs based on periodically poled lithium niobate waveguides [81]. It should be mentioned that although one-mode PSAs are not capable of modulation format independent operation they can on the other hand provide squeezing which can be used for signal regeneration [82].

4.2 Link architectures

The sub-3 dB NF of PSAs would be beneficial both in booster, inline amplifier, and preamplifier configurations [83]. However, the copier-PSA scheme only allows for certain amplifier configurations to be implemented with a performance advantage compared to conventional PIAs. In the next section we describe the copier-PSA scheme and its limitations.

4.2.1 The copier-PSA scheme

The copier-PSA scheme consists of two cascaded parametric amplifiers and is schematically illustrated in figure 4.1. The working principle, leading to modulation format independent operation and possibility of noiseless amplification, is as follows. If a signal wave and pump wave are injected into the first parametric amplifier then this amplifier, called copier, will operate in PI-mode and generate a phase-conjugated copy of the signal at the idler wavelength, as was shown in section 3.4. The second parametric amplifier will operate in PS-mode and amplify both the in-phase and quadrature components of the signal, as opposed to the

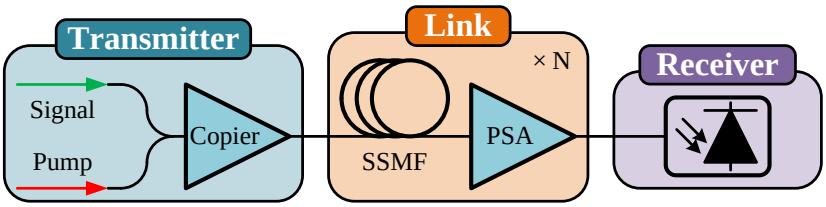

Figure 4.2: Simplified scheme for realizing PSA-amplified transmission links.

case when the idler has the same phase as the signal and one component will be attenuated.

It is clear that this scheme is modulation format independent since the signal will experience the same gain independent of its phase, leading to amplification of both signal components. The noise properties of the copier-PSA scheme are more involved and requires a more detailed discussion. Qualitatively they can be understood as follows.

We mentioned in section 3.4 that the noise associated with the signal and idler waves will be correlated at the output of a parametric amplifier [66]. The output waves from the copier will thus contain correlated noise, which in turn will prevent the PSA from noiseless amplification [66]. It is therefore essential that the noise is decorrelated before the PSA. The requirement of decorrelating the noise is what limits the possible amplifier configurations for the copier-PSA scheme. One way to decorrelate the noise is to attenuate the waves, which e.g. can be done by propagating them through an optical fiber [17, 41, 66]. A generic scheme for realizing PSA-amplified links, where the loss originate from fiber attenuation, is illustrated in figure 4.2. We note that in the case of a single span (N=1), then we get a preamplifier configuration.

Since the copier operates in PI-mode it has a quantum limited NF of 3 dB. The combined NF of the copier-PSA cascade is therefore also limited to 3 dB. This is the explanation to why the copier-PSA scheme cannot outperform an ordinary PIA when implemented in a booster configuration. For an inline and preamplifier configuration on the other hand the copier can be part of the transmitter, as illustrated in figure 4.2.

Transfer matrix description

The copier-PSA scheme can be analyzed using a transfer matrix description, similar to how we analyzed a two-mode parametric amplifier in section 3.4. On a component level the copier-PSA system consists of a two-mode PI parametric amplifier followed by a loss element, which can be treated as a beam splitter [17], followed by a two-mode PS parametric amplifier. The transfer matrix equation for

the combined systems take the form [84]

$$\begin{bmatrix} B_{\mathrm{s}} \\ B_{\mathrm{i}}^{*} \end{bmatrix} = \mathbf{G}_2 \hat{\mathbf{T}} \mathbf{G}_1 \cdot \begin{bmatrix} A_{\mathrm{s}} + n_{\mathrm{s}} \\ n_{\mathrm{i}}^{*} \end{bmatrix} \tag{4.1}$$

where A and B denote input and output modes and n_{s} and n_{i} represents the quantum noise. $\mathbf{G}_1$ and $\mathbf{G}_2$ represent the copier and PSA transfer matrices, respectively, and $\hat{\mathbf{T}}$ is an attenuation operator that satisfies

$$\hat{\mathbf{T}} \cdot \mathbf{A} = \begin{bmatrix} \sqrt{T_{\mathrm{s}}} & 0 \\ 0 & \sqrt{T_{\mathrm{s}}} \end{bmatrix} \mathbf{A} + \begin{bmatrix} \sqrt{1 - T_{\mathrm{s}}} n_{\mathrm{s}}' \\ \sqrt{1 - T_{\mathrm{i}}} n_{\mathrm{i}}' \end{bmatrix}. \tag{4.2}$$

where $\mathbf{A}$ is a vector containing two modes, e.g. the signal and idler modes after the copier. The attenuation operator works like a 4-port beam-splitter that couples quantum noise to the signal and idler [17]. The variable T denote the transmittance of the fiber and n_{s}' and n_{i}' represents quantum noise introduced by the loss process. n_{s}' and n_{i}' are uncorrelated with n_{s} and n_{i} but have the same mean value and variance.

Link noise figure

The copier-PSA scheme has been investigated based on (4.1) and it has been shown that a transmission link implementation of the scheme can give up to 6 dB link NF improvement over conventional PIA-based schemes and a 3 dB improvement over all PSA-based schemes [17, 66]. The scheme has also been investigated experimentally in a copier-loss-PSA configuration [56], i.e. the link was emulated by a lumped signal/idler loss. Based on this system amplification of dense WDM differential quadrature phase-shift keying (DQPSK) signals at 10 GBd with nearly 6 dB SNR improvement over an EDFA-based system was demonstrated [85].

In the high-gain regime the link NF for a copier-loss-PSA and PIA-loss-PIA scheme can, respectively, be written as [17]

$$\mathrm{NF}_{\text{copier-loss-PSA}} \approx 1 + \frac{G_2}{2} \quad \text{and} \quad \mathrm{NF}_{\text{PIA-loss-PIA}} \approx 1 + 2G_2 \tag{4.3}$$

where G_2 is the gain of the second amplifier. We see that at large gain ($G_2 \gg 1$) then a copier-loss-PSA link give a 6 dB NF advantage over a PIA-loss-PIA link.

In section 2.3 we compared the link NF of ideal PIA- and PSA-amplified links and reached the conclusion that the PSA-amplified link give a 3 dB improvement. The explanation to why the coper-PSA scheme give a 6 dB link NF improvement lies in the generation of the idler wave in the copier and that the idler is considered to be an internal mode of the system. If the idler power was accounted for at the input of the transmission link then a 3 dB improvement would have been obtained.

4.3 Nonlinear distortion mitigation

Due to PSAs capability of noiseless amplification most studies on PSA-amplified links have focused on the reduction of noise as a way to improve link performance. Another approach to improve performance is to reduce the impact of nonlinear distortion that follows an increase in transmitted power or transmission distance.

Several techniques for mitigation of nonlinear distortions have been proposed [86–88]. Mid-link optical phase conjugation (OPC) utilize an optical [87], or electrical [88], device to perform a phase-conjugation of the signal at the middle point of the transmission link which result in cancellation of the nonlinear phase shifts from the two halves.

In [Paper C] it was discovered that also PSAs can achieve mitigation of nonlinear distortions (SPM). The principle is based on that the PSA performs a coherent summation of the signal and conjugated signal (idler) fields that after propagation through the link will have acquired correlated nonlinear distortions. Through the coherent summation the nonlinear distortion on the two waves will cancel out which will lead to a performance improvement.

The concept of propagating a pair of phase-conjugated twin waves over a link and then perform a coherent summation to cancel nonlinear impairments can also be implemented without the use of a PSA [89, 90]. In one demonstration two polarization multiplexed phase-conjugated twin waves, generated using a dual polarization optical modulator, were transmitted over a link and summed in digital signal processing (DSP) after coherent detection [89]. In another demonstration the phase-conjugated twin waves were generated using a FOPA and after propagation detected coherently and summed in DSP [90].

4.4 Implementation challenges

In a practical realization of a PSA-amplified transmission link based on the copier-PSA scheme several stages for conditioning of the waves have to be included. A single-span PSA amplified link, including conditioning stages, is illustrated in figure 4.3. A similar figure can be found in [Paper A] and a more comprehensive discussion on the implementation challenges, than what will follow here, can be found in [Paper A-B].

The practical challenges can basically be divided into pump handling and wave tuning and stabilization. Pump handling refers to attenuating the strong pump before the transmission link, in order to avoid nonlinear effects such as XPM and SPM in the transmission fiber, and then amplifying the pump before the PSA. The low pump power at the end of the transmission span and high requirement on the pump quality in the PSA renders ordinary amplification by EDFAs impossible. The pump amplification can be achieved using an hybrid OIL/EDFA system which is discussed in [Paper A].

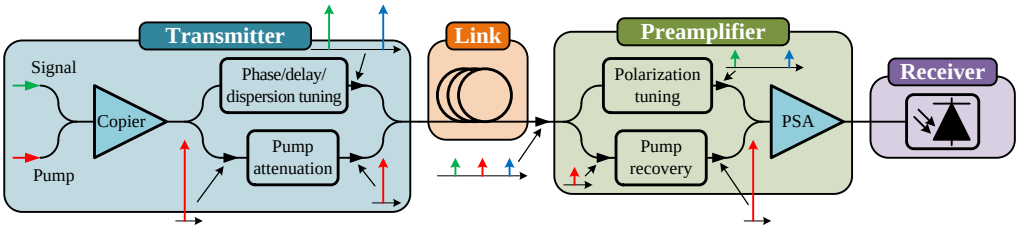

Figure 4.3: Schematic of practical realization of PSA preamplified transmission link.

Just after the copier, the signal, idler, and pump waves will be aligned with respect to polarization, phase, and time. However, after transmission the alignment will be lost and PSA amplification would not be possible it the waves were not re-aligned. In practice this means that the transmission between the copier and the PSA has to be dispersion compensated, the time delay between the waves must be tuned down to a fraction of the bit slot, and the state of polarization (SOP) of the waves must be adjusted.

Furthermore, the pump recovery system requires the signal and idler waves to be separated from the pump wave. This will result in a time dependent phase drift between the signal/idler pair and the pump wave. This phase-drift must be compensated for continuously using a phase-locked loop (PLL).

In order to demonstrate a multi-span PSA-amplified link with WDM transmission there are many technical challenges that remain. These will be discussed in chapter 6.

Chapter 5
Optical injection locking

Injection locking (IL) is a general concept that can be realized in mechanical, electrical, and optical systems. An injection-locked laser has the capability to transfer the phase information of an injected wave while suppressing the amplitude information. This property can successfully be exploited in a pump recovery system for PSA-amplified transmission links.

Chapter outline

The topic of OIL is covered at length in [Paper A] and this chapter will therefore only serve as a short introduction to the concept. In section 5.1 we give a brief account of the history of IL in general and OIL in particular and in section 5.2 we describe some of the basic concepts of OIL.

5.1 Introduction

The concept of IL describe the phenomenon when the signal from an oscillator, e.g. a mechanical oscillator, is injected into another oscillator causing the second oscillator to lock in frequency and phase to the first one. An early documented observation of this phenomenon was done by Christiaan Huygens in a letter to his father, Constantyn Huygens, in 1665 [91]. In the letter Christiaan Huygens described his observation of how the pendulums of two clocks hanging on a wall, initially swinging unsynchronized, with time became synchronized, i.e. locked in frequency and phase. He also noted that the time for reaching the synchronized state depended on the distance between the clocks. Later he concluded that the cause of synchronization was mechanical vibrations, originating from the clocks, mediated by the wall which they were hanging on.

IL can also be observed in electrical systems. An early study of IL in electronic circuits was done by Adler in 1946 when he analyzed IL of an electrical oscillator with an external frequency source [92]. In this study he derived one

of the fundamental properties of IL, for locking to occur the frequency difference between the impressed signal and the free-running oscillator cannot be too large. Adler's theory was later extended by Pantell in 1965 to include optical system, i.e. IL of lasers [93], and one year later, Stover and Steier demonstrated the first injection-locked laser using two red He-Ne lasers [94].

In the case of OIL light from one laser, termed master laser (ML), is coupled into another laser, termed slave laser (SL), which cause the frequency and phase of the SL to lock to that of the ML. OIL of semiconductor distributed feedback (DFB) lasers was first demonstrated in 1991 [95], and has since found many applications. IL can e.g. significantly enhance the performance of directly modulated DFB lasers. Noticeable results have been published on single-mode performance and enhanced side-mode suppression [96], suppressed nonlinear distortion [97], reduced frequency chirp [98], reduced relative intensity noise (RIN) and linewidth [99], enhanced resonance frequency and modulation bandwidth [100].

5.2 Basic concepts

5.2.1 Experimental implementation

There are various schemes for IL of semiconductor lasers. Two common schemes are the reflection style scheme and the transmission style scheme, illustrated in figure 5.1(a) and 5.1(b), respectively. The difference between the two schemes is in how the light is coupled in and out of the SL. In the reflection style scheme only one facet is used for coupling while in the transmission style scheme different facets are used for input and output coupling. From a practical point of view the reflection style scheme is easier to implement since the coupling can be hard, especially if it is done using free-space optics. In both schemes the ML must be isolated from the SL. In the reflection style scheme this is done by coupling the ML light into the SL via a circulator. In the transmission scheme it is accomplished by placing an isolator between the ML and the SL.

Important parameters for the locking process are the power and SOP of the light injected into the SL, the free-running output power of the SL and the free-running wavelengths of the SL and ML. For efficient locking the ML SOP has to be matched to the mode of the SL. The importance and impact of the other parameters will be discussed below.

5.2.2 Injection ratio

An important parameter for the IL process is the external injection ratio which is defined as the ratio between the power injected into the SL P_{inj} and the free-running SL output power P_{free}

$$R = \frac{P_{\text{inj}}}{P_{\text{free}}}. \tag{5.1}$$

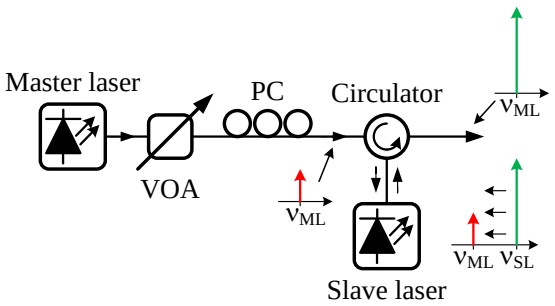

(a) Reflection style configuration

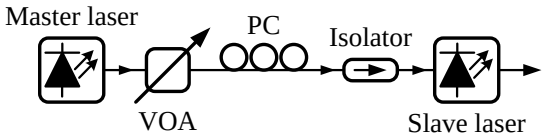

(b) Transmission style configuration

Figure 5.1: Illustration of common configurations for realizing OIL. VOA: variable optical attenuator.

The internal injection ratio is defined by instead using the injected power internal to the SL cavity and the internal power of the free-running SL. For practical reasons the external injection ratio is most common in experimental studies.

5.2.3 Locking bandwidth

The frequency difference between the injected light ν_{inj} and the free-running SL ν_{free} is also an important parameter for the locking process. Locking of the SL to the ML will only be possible within a certain range of the frequency difference $\Delta\nu = \nu_{\text{inj}} - \nu_{\text{free}}$. The range within which the locking occur is called the locking bandwidth and is determined by, among other things, the injection ratio.

5.2.4 Theoretical explanation models

Several models have been developed to describe the locking dynamics of OIL. The gain competition model was introduced in [101] and describe the competition between ASE and injected light. Another way to understand the dynamics of the OIL process is through the phasor diagram model [101]. This model describes how the steady-state is reached. The third approach is to use the rate-equations which can give us an expression for the locking bandwidth [102].

Chapter 6
Outlook

PSAs have now proved capable of outperforming EDFAs in terms of sensitivity for single-span preamplifier configurations, both in the linear [Paper B] and nonlinear [Paper C] transmission regime. These results are intriguing and motivate, by themselves, continued research on PSA-amplified transmission links. However, from a commercial perspective sensitivity is not the only measure that is important when comparing amplification technologies. Considering issues such as polarization dependent gain and the practical difficulty of ensuring that the phase relation between the waves is stable, PSAs still have a long way to go before they can be considered commercially interesting as transmission link amplifiers.

Looking beyond the issues mentioned above, some conceptually interesting and important PSA-amplified link demonstrations would be to show WDM transmission, transmission of more advanced modulation formats such as 16QAM, and multi-span transmission. The main challenge for demonstrating WDM transmission is to achieve independent polarization tuning of the WDM channels. For practical reasons a multi-span transmission experiment would preferably be carried out in a re-circulating loop configuration. Possible issues for that kind of demonstration might be noise accumulation on the pump wave and difficulties to achieve continuous phase-stabilization of the waves.

There are a few ways in which development of techniques or components could lead to better or simpler PSAs. SBS is an issue in all high-gain PSA implementations and in most cases techniques such as pump phase modulation are used to reduce the SBS. A breakthrough in SBS suppression techniques, enabling high-gain PSAs without the need of pump phase modulation, would make it possible to implement PSAs that do not suffer from broadened idler spectrum, which lead to performance degradation in some applications.

Another field where development could lead to improved PSA performance is in the field of optical fibers. New fibers with higher nonlinear coefficient and lower loss would e.g. make it possible to use shorter fibers which in turn ease the requirements on other aspects of the fiber, such as zero dispersion wavelength variations. Holey-fibers could be one such fiber type that can be used for PSAs.

Chapter 7
Summary of papers

Paper A: Injection locking-based pump recovery for phase-sensitive amplified links

Compared to conventional EDFA-amplified transmission links, PSA-amplified links would give a significant performance improvement. In order to realize PSA-amplified links with significant span lengths a pump recovery system, capable of generating a high-quality pump wave from the residual pump wave after the transmission span, is required. In this paper we demonstrate, for the first time, an IL-based pump recovery system, enabling PSA-amplified links with more than 200 km long spans. Bit error ratio (BER) measurements with 10 GBd DQPSK signals show penalty-free recovery of a pump wave, phase modulated with two sinusoidal RF-tones at 0.1 GHz and 0.3 GHz, with 64 dB amplification, from -30 dBm to 34 dBm. To understand the operating power limits for the pump recovery system the noise generation in and the phase modulation transfer through the pump recovery system is quantified and the corresponding link penalties measured and explained.

Paper B: Phase-sensitive Optical Pre-Amplifier Implemented in an 80km DQPSK Link

The ultra-low NF of PSAs makes them very attractive for use in fiber optical transmission links. There are a number of challenges in implementing a frequency-nondegenerate PSA-amplified link with a long transmission span. First of all a pump recovery system must be incorporated into the link in order to generate a high-quality pump before the PSA. In addition to this the pump, signal, and idler waves, possibly widely spaced in frequency, must be temporally synchronized after dispersion in the fiber link and tuned to have the same state of polarization at the input of the PSA. In this paper we demonstrate a record long 80 km

frequency-nondegenerate PSA-amplified transmission link. We measure 1.3 dB higher sensitivity for the PSA-amplified link compared to a comparable conventional EDFA-amplified link.

Paper C: Phase-Sensitive Amplified Optical Link Operating in the Nonlinear Transmission Regime

The key factor limiting the capacity in fiber optical transmission systems is the SNR. The SNR can be increased by launching higher signal power into the link. However, nonlinear effects set an upper bound on how high power that can be launched. In this paper we present the first characterization of a PSA-amplified link operating in the nonlinear transmission regime. We observe less nonlinear penalty in the PSA-amplified link compared to an EDFA-amplified link and also the PSA modify the distribution of nonlinear phase noise on the signal.

Bibliography

[1] T. H. Maiman, "Stimulated Optical Radiation in Ruby," Nature **187**, 493–494 (1960).

[2] K. C. Kao and G. A. Hockham, "Dielectric-fibre surface waveguides for optical frequencies," Proceedings of the Institution of Electrical Engineers **113**, 1151–1158 (1966).

[3] S. B. Poole, D. N. Payne, R. J. Mears, M. E. Fermann, and R. I. Laming, "Fabrication and Characterization of Low-Loss Optical Fibers Containing Rare-Earth Ions," Journal of Lightwave Technology **LT-4**, 870–876 (1986).

[4] T. C. Cannon, D. L. Pope, and D. D. Sell, "Installation and Performance of the Chicago Lightwave Transmission System," IEEE Transactions on Communications **COM-26**, 1056–1060 (1978).

[5] T. J. Xia, G. A. Wellbrock, A. Tanaka, M.-F. Huang, E. Ip, D. Qian, Y.-K. Huang, S. Zhang, Y. Zhang, P. N. Ji, Y. Aono, S. Murakami, and T. Tajima, "High Capacity Field Trials of 40.5 Tb/s for LH Distance of 1,822 km and 54.2 Tb/s for Regional Distance of 634 km," in "Optical Fiber Communication Conference and Exposition (OFC) and National Fiber Optic Engineers Conference (NFOEC) ," (Optical Society of America, Washington, DC, 2013), p. PDP5A.4.

[6] A. H. Gnauck, R. W. Tkach, A. R. Chraplyvy, and T. Li, "High-Capacity Optical Transmission Systems," Journal of Lightwave Technology **26**, 1032–1045 (2008).

[7] M. Hirano, T. Haruna, Y. Tamura, T. Kawano, S. Ohnuki, Y. Yamamoto, Y. Koyano, and T. Sasaki, "Record Low Loss, Record High FOM Optical Fiber with Manufacturable Process," in "Optical Fiber Communication Conference and Exposition (OFC) and National Fiber Optic Engineers Conference (NFOEC) ," (Optical Society of America, Washington, DC, 2013), p. PDP5A.7.

[8] C. E. Shannon, "Communication in the Presence of Noise," Proceedings of the IRE **37**, 10–21 (1949).

[9] E. Desurvire, *Erbium-doped Fiber Amplifiers* (John Wiley & Sons, 1994).

[10] R. I. Laming, M. N. Zervas, and D. N. Payne, "Erbium-Doped Fiber Amplifier with 54 dB Gain and 3.1 dB Noise Figure," IEEE Photonics Technology Letters **4**, 1345–1347 (1992).

[11] C. M. Caves, "Quantum limits on noise in linear amplifiers," Physical Review D **26**, 1817–1839 (1982).

[12] H. Masuda, S. Kawai, and K. I. Suzuki, "Optical SNR enhanced amplification in long-distance recirculating-loop WDM transmission experiment using 1580 nm band hybrid amplifier," Electronics Letters **35**, 411–412 (1999).

[13] E. Pincemin, T. Guillossou, N. Evanno, S. Lobanov, and S. Ten, "Record transmission distances over Ultra Low Loss G.652 fibre with NRZ-OOK or NRZ-DPSK 40 Gbps WDM systems," in "Optical Fiber Communication Conference and Exposition (OFC) and National Fiber Optic Engineers Conference (NFOEC) ," (Optical Society of America, Washington, DC, 2009), p. OThC2.

[14] T. Torounidis, P. A. Andrekson, and B.-E. Olsson, "Fiber-Optical Parametric Amplifier With 70-dB Gain," IEEE Photonics Technology Letters **18**, 1194–1196 (2006).

[15] J. Hansryd, P. A. Andrekson, M. Westlund, J. Li, and P.-O. Hedekvist, "Fiber-Based Optical Parametric Amplifiers and Their Applications," IEEE Journal of Selected Topics in Quantum Electronics**8**, 506–520 (2002).

[16] R. Tang, J. Lasri, P. S. Devgan, V. Grigoryan, P. Kumar, and M. Vasilyev, "Gain characteristics of a frequency nondegenerate phase-sensitive fiber-optic parametric amplifier with phase self-stabilized input," Optics Express **13**, 10483–10493 (2005).

[17] C. J. McKinstrie, M. Karlsson, and Z. Tong, "Field-quadrature and photon-number correlations produced by parametric processes," Optics Express **18**, 19792–19823 (2010).

[18] E. Lach and W. Idler, "Modulation formats for 100G and beyond," Optical Fiber Technology **17**, 377–386 (2011).

[19] H. Heffner, "The Fundamental Noise Limit of Linear Amplifiers," Proceedings of the IRE pp. 1604–1608 (1962).

[20] H. A. Haus and J. A. Mullen, "Quantum Noise in Linear Amplifiers," Physical Review **128**, 2407–2413 (1962).

[21] R. J. Mears, L. Reekie, I. M. Jauncey, and D. N. Payne, "Low-noise erbium-doped fibre amplifier operating at 1.54μm," Electronics Letters **23**, 1026–1028 (1987).

[22] M. N. Islam, "Raman Amplifiers for Telecommunications," IEEE Journal of Selected Topics in Quantum Electronics**8**, 493–494 (2002).

[23] M. J. Connelly, *Semiconductor Optical Amplifiers* (Kluwer, 2004).

[24] F. A. Flood, "L-Band Erbium-Doped Fiber Amplifiers," in "Optical Fiber Communication Conference and Exposition (OFC) and National Fiber Optic

Engineers Conference (NFOEC) ," (Optical Society of America, Washington, DC, 2000), pp. WG1–2.

[25] J. B. Rosolem and A. A. Juriollo, "S Band EDFA Using Standard Erbium Doped Fiber, 1450 nm Pumping and Single Stage ASE Filtering," in "Optical Fiber Communication Conference and Exposition (OFC) and National Fiber Optic Engineers Conference (NFOEC) ," (Optical Society of America, Washington, DC, 2008), p. OTuN3.

[26] S. Aozasa, H. Masuda, H. Ono, T. Sakamoto, T. Kanamori, Y. Ohishi, and M. Shimizu, "1480-1510 nm-band Tm doped fiber amplifier (TDFA) with a high power conversion efficiency of 42 %," in "Optical Fiber Communication Conference and Exposition (OFC) and National Fiber Optic Engineers Conference (NFOEC) ," (Optical Society of America, Washington, DC, 2001), pp. PD1–3.

[27] J. Bromage, "Raman Amplification for Fiber Communications Systems," Journal of Lightwave Technology **22**, 79–93 (2004).

[28] X. Li and G. Li, "Electrical Postcompensation of SOA Impairments for Fiber-Optic Transmission," IEEE Photonics Technology Letters **21**, 581–583 (2009).

[29] A. E. Kelly, I. F. Lealman, L. J. Rivers, S. D. Perrin, and M. Silver, "Low noise figure (7.2 dB) and high gain (29 dB) semiconductor optical amplifier with a single layer AR coating," Electronics Letters **33**, 536–538 (1997).

[30] E. J. Woodbury and W. K. Ng, "Ruby Laser Operating in the Near IR," Proceedings of the IRE **50**, 2367 (1962).

[31] G. Eckhardt, R. W. Hellwarth, F. J. McClung, S. E. Schwarz, D. Weiner, and E. J. Woodbury, "Stimulated raman scattering from organic liquids," Physical Review Letters **9**, 455–457 (1962).

[32] R. H. Stolen and E. P. Ippen, "Raman gain in glass optical waveguides," Applied Physics Letters **22**, 276–278 (1973).

[33] C. V. Raman and K. S. Krishnan, "A New Type of Secondary Radiation," Nature **121**, 501–502 (1928).

[34] E. Desurvire, M. Papuchon, J. P. Pocholle, and J. Raffy, "High-gain optical amplification of laser diode signal by Raman scattering in single-mode fibres," Electronics Letters **19**, 751–753 (1983).

[35] R. Loudon, *The quantum theory of light* (Oxford University Press, 2000).

[36] D. Marcuse, *Principles of quantum electronics* (Academic press, 1980).

[37] Y. Yamamoto and K. Inoue, "Noise in Amplifiers," Journal of Lightwave Technology **21**, 2895–2915 (2003).

[38] J. J. Sakurai, *Modern Quantum Mechanics* (Addison Wesley Longman, 1994).

[39] H. T. Friis, "Noise Figures of Radio Receivers," Proceedings of the IRE **32**, 419–422 (1944).

[40] R. Loudon, "Theory of Noise Accumulation in Linear Optical-Amplifier Chains," IEEE Journal of Quantum Electronics **QE-21**, 766–773 (1985).

[41] Z. Tong, C. J. McKinstrie, C. Lundström, M. Karlsson, and P. A. Andrekson, "Noise performance of optical fiber transmission links that use non-degenerate cascaded phasesensitive amplifiers," Optics Express **18**, 15426–15439 (2010).

[42] D. F. Walls, "Squeezed states of light," Nature **306**, 141–146 (1983).

[43] G. P. Agrawal, *Nonlinear Fiber Optics, 5th Ed.* (Academic Press, 2012).

[44] J. A. Armstrong, N. Bloembergen, J. Ducuing, and P. S. Pershan, "Interactions between Light Waves in a Nonlinear Dielectric," Physical Review **127**, 1918–1939 (1962).

[45] N. M. Kroll, "Parametric Amplification in Spatially Extended Media and Application to the Design of Tuneable Oscillators at Optical Frequencies," Physical Review **127**, 1207–1211 (1962).

[46] S.-K. Choi, R.-D. Li, C. Kim, and P. Kumar, "Traveling-wave optical parametric amplifier: investigation of its phase-sensitive and phase-insensitive gain response," Journal of the Optical Society of America B **14**, 1564–1575 (1997).

[47] D. J. Lovering, J. A. Levenson, P. Vidakovic, J. Webjörn, and P. S. J. Russell, "Noiseless optical amplification in quasi-phase-matched bulk lithium niobate," *Opt. Lett.***21**, 1439–1441 (1996).

[48] R. H. Stolen, "Phase-Matched-Stimulated Four-Photon Mixing in Silica-Fiber Waveguides," IEEE Journal of Quantum Electronics **QE-11**, 100–103 (1975).

[49] R. H. Stolen and J. E. Bjorkholm, "Parametric Amplification and Frequency Conversion in Optical Fibers," IEEE Journal of Quantum Electronics **QE-17**, 1062–1072 (1982).

[50] C. Lin, W. A. Reed, A. D. Pearson, and H. T. Shang, "Phase matching in the minimum-chromatic-dispersion region of single-mode fibers for stimulated four-photon mixing," Optics Letters **6**, 493–495 (1981).

[51] K. Washio, K. Inoue, and S. Kishida, "Efficient large-frequency-shifted three-wave mixing in low dispersion wavelength region in single-mode optical fibre," Electronics Letters **16**, 658–660 (1980).

[52] F. Yang, M. Marhic, and L. Kazovsky, "CW fibre optical parametric amplifier with net gain and wavelength conversion efficiency > 1," Electronics Letters **32**, 2336–2338 (1996).

[53] J. Hansryd and P. A. Andrekson, "Broad-Band Continuous-Wave-Pumped Fiber Optical Parametric Amplifier with 49-dB Gain and Wavelength-Conversion Efficiency," IEEE Photonics Technology Letters **13**, 194–196 (2001).

[54] J. C. Boggio, C. Lundström, J. Yang, H. Sunnerud, and P. Andrekson, "Double-pumped FOPA with 40 dB flat gain over 81 nm bandwidth," in

"European Conference and Exhibition on Optical Communication (ECOC) ," (Optical Society of America, Washington, DC, 2008), p. Tu.3.B.5.

[55] P. L. Voss, R. Tang, and P. Kumar, "Measurement of the photon statistics and the noise figure of a fiber-optic parametric amplifier," Optics Letters **28**, 549–551 (2003).

[56] Z. Tong, C. Lundström, P. A. Andrekson, C. J. McKinstrie, M. Karlsson, D. J. Blessing, E. Tipsuwannakul, B. J. Puttnam, H. Toda, and L. Grüner-Nielsen, "Towards ultrasensitive optical links enabled by low-noise phase-sensitive amplifiers," Nature Photonics **5**, 430–436 (2011).

[57] P. A. Andrekson, "Picosecond optical sampling using four-wave mixing in fibre," Electronics Letters **27**, 1440–1441 (1991).

[58] P. A. Andrekson, N. A. Olsson, J. R. Simpson, T. Tanbun-ek, R. A. Logan, and M. Haner, "16 Gbit/s all-optical demultiplexing using four-wave mixing," Electronics Letters **27**, 922–924 (1991).

[59] K. Inoue, "Optical level equalisation based on gain saturation in fibre optical parametric amplifier," Electronics Letters **36**, 1016–1017 (2000).

[60] G.-W. Lu and T. Miyazaki, "Optical phase erasure based on FWM in HNLF enabling format conversion from 320-Gb/s RZDQPSK to 160-Gb/s RZ-DPSK," Optics Express **17**, 13346–13353 (2009).

[61] R. Jopson and R. Tench, "Polarisation-independent phase conjugation of lightwave signals," Electronics Letters **29**, 2216–2217 (1993).

[62] K. Inoue, "Polarization Independent Wavelength Conversion Using Fiber Four-Wave Mixing with Two Orthogonal Pump Lights of Different Frequencies," Journal of Lightwave Technology **12**, 1916–1920 (1994).

[63] M. O. van Deventer, *Fundamentals of Bidirectional Transmission over a Single Optical Fibre*, vol. 2 of *Solid-State Science and Technology Library* (Springer, 1996).

[64] C. J. McKinstrie, S. Radic, and M. G. Raymer, "Quantum noise properties of parametric amplifiers driven by two pump waves," Optics Express **12**, 5037–5066 (2004).

[65] M. Vasilyev, "Distributed phase-sensitive amplification," Optics Express **13**, 7563–7571 (2005).

[66] Z. Tong, A. Bogris, C. Lundström, C. J. McKinstrie, M. Vasilyev, M. Karlsson, and P. A. Andrekson, "Modeling and measurement of the noise figure of a cascaded non-degenerate phase-sensitive parametric amplifier," Optics Express **18**, 14820–14835 (2010).

[67] M. Hirano, T. Nakanishi, T. Okuno, and M. Onishi, "Silica-Based Highly Nonlinear Fibers and Their Application," IEEE Journal of Selected Topics in Quantum Electronics**15**, 103–113 (2009).

[68] S. K. Korotky, P. B. Hansen, L. Eskildsen, and J. J. Veselka, "Efficient phase modulation scheme for suppressing stimulated brillouin scattering,"

in "Proc. Technol. Dig. Conf. Integr. Opt. Fiber Commun.", (1995), pp. 110–111.

[69] C. Lundström, R. Malik, L. Grüner-Nielsen, B. Corcoran, S. L. I. Olsson, M. Karlsson, and P. A. Andrekson, "Fiber Optic Parametric Amplifier With 10-dB Net Gain Without Pump Dithering," IEEE Photonics Technology Letters **25**, 234–237 (2013).

[70] H. P. Yuen, "Design of transparent optical networks by using novel quantum amplifiers and sources," Optics Letters **12**, 789–791 (1987).

[71] M. Shirasaki and H. A. Haus, "Squeezing of pulses in a nonlinear interferometer," Journal of the Optical Society of America B **7**, 30–34 (1990).

[72] M. E. Marhic, C. H. Hsia, and J. M. Jeong, "Optical amplification in a nonlinear fibre interferometer," Optics Letters **27**, 210–211 (1991).

[73] W. Imajuku and A. Takada, "Error-free operation of in-line phase-sensitive amplifier," Electronics Letters **34**, 1673–1674 (1998).

[74] J. Kakande, C. Lundström, P. A. Andrekson, Z. Tong, M. Karlsson, P. Petropoulos, F. Parmigiani, and D. J. Richardson, "Detailed characterization of a fiber-optic parametric amplifier in phase-sensitive and phase-insensitive operation," Optics Express **18**, 4130–4137 (2010).

[75] I. Bar-Joseph, A. A. Friesem, R. G. Waarts, and H. H. Yaffe, "Parametric interaction of a modulated wave in a single-mode fiber," Optics Letters **11**, 534–536 (1986).

[76] R. Tang, P. Devgan, V. S. Grigoryan, and P. Kumar, "Inline frequency-nondegenerate phase-sensitive fibre parametric amplifier for fibre-optic communication," Electronics Letters **41**, 1072–1074 (2005).

[77] R. Tang, P. Devgan, P. L. Voss, V. S. Grigoryan, and P. Kumar, "In-Line Frequency-Nondegenerate Phase-Sensitive Fiber-Optical Parametric Amplifier," IEEE Photonics Technology Letters **17**, 1845–1847 (2005).

[78] O. K. Lim, V. Grigoryan, M. Shin, and P. Kumar, "Ultra-Low-Noise Inline Fiber-Optic Phase-Sensitive Amplifier for Analog Optical Signals," in "Optical Fiber Communication Conference and Exposition (OFC) and National Fiber Optic Engineers Conference (NFOEC) ," (Optical Society of America, Washington, DC, 2008), p. OML3.

[79] R. Tang, P. S. Devgan, V. S. Grigoryan, P. Kumar, and M. Vasilyev, "In-line phase-sensitive amplification of multichannel CW signals based on frequency nondegenerate four-wave-mixing in fiber," Optics Express **16**, 9046–9053 (2008).

[80] R. Tang, M. Shin, P. Devgan, V. S. Grigoryan, M. Vasilyev, and P. Kumar, "Toward in-line phase-sensitive fiber-parametric amplification of multichannel signals," in "Conference on Lasers and Electro-Optics (CLEO) ," (Optical Society of America, Washington, DC, 2006), p. JThC81.

[81] T. Umeki, M. Asobe, H. Takara, Y. Miyamoto, and H. Takenouchi, "Multi-span transmission using phase and amplitude regeneration in PPLN-based PSA," Optics Express **21**, 18170–18177 (2013).

[82] R. Slavík, F. Parmigiani, J. Kakande, C. Lundström, M. Sjödin, P. A. Andrekson, R. Weerasuriya, S. Sygletos, A. D. Ellis, L. Grüner-Nielsen, D. Jakobsen, S. Herstrøm, R. Phelan, J. O′Gorman, A. Bogris, D. Syvridis, S. Dasgupta, P. Petropoulos, and D. J. Richardson, "All-optical phase and amplitude regenerator for next-generation telecommunications systems," Nature Photonics **4**, 690–695 (2010).

[83] Y. Yamamoto and T. Mukai, "Fundamentals of optical amplifiers," Optical and Quantum Elecctronics **21**, S1–S14 (1989).

[84] Z. Tong, C. Lundström, P. A. Andrekson, M. Karlsson, and A. Bogris, "Ultralow Noise, Broadband Phase-Sensitive Optical Amplifiers, and Their Applications," IEEE Journal of Selected Topics in Quantum Electronics**18**, 1016–1032 (2012).

[85] Z. Tong, C. Lundström, E. Tipsuwannakul, M. Karlsson, and P. A. Andrekson, "Phase-Sensitive Amplified DWDM DQPSK Signals Using Free-Running Lasers with 6-dB Link SNR Improvement over EDFA-based Systems," in "European Conference and Exhibition on Optical Communication (ECOC) ," (Optical Society of America, Washington, DC, 2010), p. PDP1.3.

[86] E. Ip and J. M. Kahn, "Compensation of Dispersion and Nonlinear Impairments Using Digital Backpropagation," Journal of Lightwave Technology **26**, 3416–3425 (2008).

[87] S. L. Jansen, D. van den Borne, B. Spinnler, S. Calabrò, H. Suche, P. M. Krummrich, W. Sohler, G.-D. Khoe, and H. de Waardt, "Optical Phase Conjugation for Ultra Long-Haul Phase-Shift-Keyed Transmission," Journal of Lightwave Technology **24**, 54–64 (2006).

[88] E. F. Mateo, X. Zhou, and G. Li, "Electronic phase conjugation for nonlinearity compensation in fiber communication systems," in "Optical Fiber Communication Conference and Exposition (OFC) and National Fiber Optic Engineers Conference (NFOEC) ," (Optical Society of America, Washington, DC, 2011), p. JWA25.

[89] X. Liu, A. R. Chraplyvy, P. J. Winzer, R. W. Tkach, and S. Chandrasekhar, "Phase-conjugated twin waves for communication beyond the Kerr nonlinearity limit," Nature Photonics **7**, 560–568 (2013).

[90] Y. Tian, Y.-K. Huang, S. Zhang, P. R. Prucnal, , and T. Wang, "Demonstration of digital phase-sensitive boosting to extend signal reach for long-haul WDM systems using optical phase-conjugated copy," Optics Express **21**, 5099–5106 (2013).

[91] A. Pikovsky, M. Rosenblum, and J. Kurths, *Synchronization: A Universal Concept in Nonlinear Sciences*, vol. 12 of *Cambridge Nonlinear Science Series* (Cambridge University Press, 2003).

[92] R. Adler, "A Study of Locking Phenomena in Oscillators," Proceedings of the IRE **34**, 351–357 (1946).

[93] R. H. Pantell, "The Laser Oscillator with an External Signal," Proceedings of the IEEE **53**, 474–477 (1965).

[94] H. L. Stover and W. H. Steier, "Locking of laser oscillators by light injection," Applied Physics Letters **8**, 91–93 (1966).

[95] R. Hui, A. D'Ottavi, A. Mecozzi, and P. Spano, "Injection Locking in Distributed Feedback Semiconductor Lasers," IEEE Journal of Quantum Electronics **27**, 1688–1695 (1991).

[96] K. Iwashita and K. Nakagawa, "Suppression of Mode Partition Noise by Laser Diode Light Injection," IEEE Journal of Quantum Electronics **QE-18**, 1669–1674 (1982).

[97] X. J. Meng, T. Chau, D. T. K. Tong, and M. Wu, "Suppression of second harmonic distortion in directly modulated distributed feedback lasers by external light injection," Electronics Letters **34**, 2040–2041 (1998).

[98] C. Lin and F. Mengel, "Reduction of frequency chirping and dynamic linewidth in high-speed directly modulated semiconductor lasers by injection locking," Electronics Letters **20**, 1073–1075 (1984).

[99] N. Schunk and K. Petermann, "Noise Analysis of Injection-Locked Semiconductor Injection Lasers," IEEE Journal of Quantum Electronics **QE-22**, 642–650 (1986).

[100] E. K. Lau, L. J. Wong, X. Zhao, Y.-K. Chen, C. J. Chang-Hasnain, and M. C. Wu, "Bandwidth Enhancement by Master Modulation of Optical Injection-Locked Lasers," Journal of Lightwave Technology **26**, 2584–2593 (2008).

[101] C. H. Henry, N. A. Olsson, and N. K. Dutta, "Locking Range and Stability of Injection Locked 1.54 μm InGaAsP Semiconductor Lasers," IEEE Journal of Quantum Electronics **QE-21**, 1152–1156 (1985).

[102] R. Lang, "Injection Locking Properties of a Semiconductor Laser," IEEE Journal of Quantum Electronics **QE-18**, 976–983 (1982).

Appendix A
Derivations

A.1 Derivation of $B_+(A_+)$ and $B_-(A_-)$

We take our starting point in (3.19)

$$\begin{cases} A_+ = \dfrac{A_\mathrm{s} + A_\mathrm{i}}{\sqrt{2}} \\ A_- = \dfrac{A_\mathrm{s} - A_\mathrm{i}}{\sqrt{2}} \end{cases} \tag{A.1}$$

$$\Rightarrow$$

$$\begin{cases} A_\mathrm{s} = \dfrac{A_+ + A_-}{\sqrt{2}} \\ A_\mathrm{i} = \dfrac{A_+ - A_-}{\sqrt{2}} \end{cases} \tag{A.2}$$

We can now define B_+ and B_- and show (3.20) using (3.18) and (A.2). We get

$$\begin{aligned} B_+ &= \frac{B_\mathrm{s} + B_\mathrm{i}}{\sqrt{2}} = \frac{\mu A_\mathrm{s} + \nu A_\mathrm{i}^* + \nu A_\mathrm{s}^* + \mu A_\mathrm{i}}{\sqrt{2}} \\ &= \frac{\mu(A_+ + A_-) + \nu(A_+ - A_-)^* + \nu(A_+ + A_-)^* + \mu(A_+ - A_-)}{2} \\ &= \mu A_+ + \nu A_+^* \end{aligned} \tag{A.3}$$

and

$$\begin{aligned} B_- &= \frac{B_\mathrm{s} - B_\mathrm{i}}{\sqrt{2}} = \frac{\mu A_\mathrm{s} + \nu A_\mathrm{i}^* - (\nu A_\mathrm{s}^* + \mu A_\mathrm{i})}{\sqrt{2}} \\ &= \frac{\mu(A_+ + A_-) + \nu(A_+ - A_-)^* - \left[\nu(A_+ + A_-)^* + \mu(A_+ - A_-)\right]}{2} \\ &= \mu A_- - \nu A_-^*. \end{aligned} \tag{A.4}$$

A.2 Derivation of $B_+(A_{\mathbf{r},+})$ and $B_-(A_{\mathbf{r},-})$

$$
\begin{aligned}
B_+ &= \mu A_+ + \nu A_+^* = |\mu|\exp(i\theta_\mu)A_+ + |\nu|\exp(i\theta_\nu)A_+^* = \left[\theta_{\mathrm{r}}^+ = \frac{\theta_\mu + \theta_\nu}{2}\right] = \\
&= \exp(i\theta_{\mathrm{r}}^+)\left[|\mu|\exp\left(i\frac{2\theta_\mu - \theta_\mu - \theta_\nu}{2}\right)A_+ + |\nu|\exp\left(i\frac{2\theta_\nu - \theta_\mu - \theta_\nu}{2}\right)A_+^*\right] \\
&= \left[\theta_{\mathrm{r}}^- = \frac{\theta_\mu - \theta_\nu}{2}\right] = \exp(i\theta_{\mathrm{r}}^+)\Big[|\mu|\exp(i\theta_{\mathrm{r}}^-)A_+ + |\nu|\exp(-i\theta_{\mathrm{r}}^-)A_+^*\Big] = \\
&= \Big[A_{\mathrm{r},+} = A_+ n\exp(i\theta_{\mathrm{r}}^-)\Big] = \exp(i\theta_{\mathrm{r}}^+)\Big(|\mu|A_{\mathrm{r},+} + |\nu|A_{\mathrm{r},+}^*\Big) = \\
&= \exp(i\theta_{\mathrm{r}}^+)\Big\{|\mu|\big[\mathrm{Re}(A_{\mathrm{r},+}) + i\mathrm{Im}(A_{\mathrm{r},+})\big] + |\nu|\big[\mathrm{Re}(A_{\mathrm{r},+}) - i\mathrm{Im}(A_{\mathrm{r},+})\big]\Big\} \\
&= \exp(i\theta_{\mathrm{r}}^+)\Big[(|\mu| + |\nu|)\mathrm{Re}(A_{\mathrm{r},+}) + i(|\mu| - |\nu|)\mathrm{Im}(A_{\mathrm{r},+})\Big]
\end{aligned}
\tag{A.5}
$$

$$
\begin{aligned}
B_- &= \mu A_- - \nu A_-^* = |\mu|\exp(i\theta_\mu)A_- - |\nu|\exp(i\theta_\nu)A_-^* = \left[\theta_{\mathrm{r}}^+ = \frac{\theta_\mu + \theta_\nu}{2}\right] = \\
&= \exp(i\theta_{\mathrm{r}}^+)\left[|\mu|\exp\left(i\frac{2\theta_\mu - \theta_\mu - \theta_\nu}{2}\right)A_- - |\nu|\exp\left(i\frac{2\theta_\nu - \theta_\mu - \theta_\nu}{2}\right)A_-^*\right] \\
&= \left[\theta_{\mathrm{r}}^- = \frac{\theta_\mu - \theta_\nu}{2}\right] = \exp(i\theta_{\mathrm{r}}^+)\Big[|\mu|\exp(i\theta_{\mathrm{r}}^-)A_- - |\nu|\exp(-i\theta_{\mathrm{r}}^-)A_-^*\Big] = \\
&= \Big[A_{\mathrm{r},\text{-}} = A_-\exp(i\theta_{\mathrm{r}}^-)\Big] = \exp(i\theta_{\mathrm{r}}^+)\Big(|\mu|A_{\mathrm{r},\text{-}} - |\nu|A_{\mathrm{r},\text{-}}^*\Big) = \\
&= \exp(i\theta_{\mathrm{r}}^+)\Big\{|\mu|\big[\mathrm{Re}(A_{\mathrm{r},\text{-}}) + i\mathrm{Im}(A_{\mathrm{r},\text{-}})\big] - |\nu|\big[\mathrm{Re}(A_{\mathrm{r},\text{-}}) - i\mathrm{Im}(A_{\mathrm{r},\text{-}})\big]\Big\} \\
&= \exp(i\theta_{\mathrm{r}}^+)\Big[(|\mu| - |\nu|)\mathrm{Re}(A_{\mathrm{r},\text{-}}) + i(|\mu| + |\nu|)\mathrm{Im}(A_{\mathrm{r},\text{-}})\Big]
\end{aligned}
\tag{A.6}
$$